Missouri State University

BearWorks

College of Natural and Applied Sciences

2010

First Kepler results on compact pulsators - I. Survey target selection and the first pulsators

R H. Østensen

R. Silvotti

S. Charpinet

R. Oreiro

G. Handler

See next page for additional authors

Follow this and additional works at: https://bearworks.missouristate.edu/articles-cnas

Recommended Citation

Østensen, Roy H., Roberto Silvotti, S. Charpinet, R. Oreiro, Gerald Handler, E. M. Green, Steven Bloemen et al. "First Kepler results on compact pulsators–I. Survey target selection and the first pulsators." Monthly Notices of the Royal Astronomical Society 409, no. 4 (2010): 1470-1486.

This article or document was made available through BearWorks, the institutional repository of Missouri State University. The work contained in it may be protected by copyright and require permission of the copyright holder for reuse or redistribution.
For more information, please contact BearWorks@library.missouristate.edu.

Authors

R H. Østensen; R. Silvotti; S. Charpinet; R. Oreiro; G. Handler; E. M. Green; S. Bloemen; U. Heber; Michael D. Reed; and For complete list of authors, see publisher's website.

This article is available at BearWorks: https://bearworks.missouristate.edu/articles-cnas/504

Monthly Notices
of the
ROYAL ASTRONOMICAL SOCIETY

Mon. Not. R. Astron. Soc. **409,** 1470–1486 (2010) doi:10.1111/j.1365-2966.2010.17366.x

First *Kepler* results on compact pulsators – I. Survey target selection and the first pulsators

R. H. Østensen,[1⋆] R. Silvotti,[2] S. Charpinet,[3] R. Oreiro,[1,4] G. Handler,[5] E. M. Green,[6] S. Bloemen,[1] U. Heber,[7] B. T. Gänsicke,[8] T. R. Marsh,[8] D. W. Kurtz,[9] J. H. Telting,[10] M. D. Reed,[11] S. D. Kawaler,[12] C. Aerts,[1,13] C. Rodríguez-López,[3,14] M. Vučković,[1,15] T. A. Ottosen,[10,16] T. Liimets,[10,17] A. C. Quint,[11] V. Van Grootel,[3] S. K. Randall,[18] R. L. Gilliland,[19] H. Kjeldsen,[15] J. Christensen-Dalsgaard,[15] W. J. Borucki,[20] D. Koch[20] and E. V. Quintana[21]

[1]*Instituut voor Sterrenkunde, K.U. Leuven, Celestijnenlaan 200D, 3001 Leuven, Belgium*
[2]*INAF-Osservatorio Astronomico di Torino, Strada dell'Osservatorio 20, 10025 Pino Torinese, Italy*
[3]*Laboratoire d'Astrophysique de Toulouse–Tarbes, Université de Toulouse, 14 avenue, Edouard Belin, Toulouse 31400, France*
[4]*Instituto de Astrofísica de Andalucía, Glorieta de la Astronomía s/n, 18008 Granada, Spain*
[5]*Institut für Astronomie, Universität Wien, Türkenschanzstrasse 17, 1180 Wien, Austria*
[6]*Steward Observatory, University of Arizona, 933 N. Cherry Avenue, Tucson, AZ 85721, USA*
[7]*Dr. Karl Remeis-Observatory & ECAP, Astronomical Institute, FAU Erlangen-Nürnberg, Sternwartstrasse 7, 96049 Bamberg, Germany*
[8]*Department of Physics, University of Warwick, Coventry CV4 7AL*
[9]*Jeremiah Horrocks Institute of Astrophysics, University of Central Lancashire, Preston PR1 2HE*
[10]*Nordic Optical Telescope, 38700 Santa Cruz de La Palma, Spain*
[11]*Department of Physics, Astronomy, and Materials Science, Missouri State University, Springfield, MO 65897, USA*
[12]*Department of Physics and Astronomy, Iowa State University, Ames, IA 50011, USA*
[13]*Department of Astrophysics, IMAPP, Radboud University Nijmegen, 6500 GL Nijmegen, the Netherlands*
[14]*Departemento de Física Aplicada, Universidad de Vigo, Campus Lagoas-Marcosende s/n, 36310 Vigo, Spain*
[15]*European Southern Observatory, Alonso de Córdova 3107, Vitacura, Casilla 19001, Santiago, Chile*
[16]*Department of Physics and Astronomy, Aarhus University, 8000 Aarhus C, Denmark*
[17]*Tartu Observatoorium, Tõravere 61602, Estonia*
[18]*ESO, Karl-Schwarzschild Strasse 2, 85748 Garching bei München, Germany*
[19]*Space Telescope Science Institute, 3700 San Martin Drive, Baltimore, MD 21218, USA*
[20]*NASA Ames Research Center, MS 244-30, Moffett Field, CA 94035, USA*
[21]*SETI Institute, NASA Ames Research Center, MS 244-30, Moffett Field, CA 94035, USA*

Accepted 2010 July 14. Received 2010 July 12; in original form 2010 June 7

ABSTRACT

We present results from the first two quarters of a survey to search for pulsations in compact stellar objects with the *Kepler* spacecraft. The survey sample and the various methods applied in its compilation are described, and spectroscopic observations are presented to separate the objects into accurate classes. From the *Kepler* photometry we clearly identify nine compact pulsators and a number of interesting binary stars. Of the pulsators, one shows the strong, rapid pulsations typical of a V361 Hya-type sdB variable (sdBV); seven show long-period pulsation characteristics of V1093 Her-type sdBVs; and one shows low-amplitude pulsations with both short and long periods. We derive effective temperatures and surface gravities for all the subdwarf B stars in the sample and demonstrate that below the boundary region where hybrid sdB pulsators are found, all our targets are pulsating. For the stars hotter than this boundary temperature a low fraction of strong pulsators (<10 per cent) is confirmed. Interestingly, the short-period pulsator also shows a low-amplitude mode in the long-period region, and several of the V1093 Her pulsators show low-amplitude modes in the short-period region, indicating that hybrid behaviour may be common in these stars, also outside the boundary temperature region where hybrid pulsators have hitherto been found.

Key words: surveys – binaries: close – stars: oscillations – subdwarfs – white dwarfs.

⋆E-mail: roy@ster.kuleuven.be

© 2010 The Authors. Journal compilation © 2010 RAS

Downloaded from https://academic.oup.com/mnras/article-abstract/409/4/1470/984924 by guest on 29 April 2020

1 INTRODUCTION

Among the different classes of pulsating stars, the various subclasses of hot subdwarfs and white dwarfs show comparable observational characteristics, with pulsation periods that can be as short as ∼1 min, due to the compact nature of these objects (Aerts, Christensen-Dalsgaard & Kurtz 2010). The term *compact pulsators*, used in this series of articles, refers to all these compact oscillating stars as a group. However, in the first half of the survey phase of the *Kepler Mission,* no strongly pulsating white dwarfs (WDs) were found, and for this reason we will concentrate primarily on the pulsating subdwarf B (sdB) stars, of which we have identified nine clear cases.

Most sdBs are extreme horizontal branch (EHB) stars, which identifies them as core helium-burning post-RGB stars with a mass close to the helium flash mass of 0.5 $M_\odot$, and hydrogen envelopes too thin to sustain shell burning. In order for them to reach this configuration, an extraordinary mechanism is required to remove almost the entire envelope when they are close to the tip of the RGB. Three distinct scenarios involving binary interactions have been identified and found to be sufficient to establish the EHB stars as the cause of the UV-upturn phenomenon seen in elliptical galaxies (see Podsiadlowski et al. 2008, for a review). But many questions remain, both with respect to the contributions from the different binary channels and especially regarding the creation of single sdB stars.

Pulsations in sdB stars were discovered by Kilkenny et al. (1997) and they are now known as sdBV stars or V361 Hya stars, after the prototype (EC 14026−2647). These stars are multiperiodic pulsators with very short periods, typically 2–3 min, and have effective temperatures between 28 000 and 37 000 K and surface gravities typically between $\log g$ [cgs] = 5.5 and 6.1 (Østensen et al. 2010a). Some years after the discovery of short-period pulsations, Green et al. (2003) reported pulsations with much longer periods (∼1 h) in sdB stars with temperatures below ∼30 000 K.[1] These stars are often referred to as long-period sdBVs or V1093 Her stars after the prototype. More recently, Schuh et al. (2006) found a star on the boundary between the V361 Hya and V1093 Her stars that exhibits simultaneous short- and long-period pulsations. Such hybrid pulsators are often referred to as DW Lyn stars after the prototype. Now, four stars in this temperature boundary region have been found with both types of pulsations. In addition to DW Lyn they are Balloon 090100001 (Oreiro et al. 2004, 2005), V391 Peg (Østensen et al. 2001b; Lutz et al. 2009) and RAT 0455+1305 (Ramsay et al. 2006; Baran & Fox Machado 2010). With the exception of V338 Ser, all pulsating sdB stars reside on or very close to the canonical Extreme Horizontal Branch (see Charpinet et al. 2009; Heber 2009; Østensen 2009 for recent detailed reviews of asteroseismology of EHB stars and hot subdwarfs in general).

Due to the recent discoveries of various subclasses of pulsators in the sdB family, a common nomenclature has yet to emerge. Kilkenny et al. (2010) have recently proposed to label the different types of sdBV stars with subscripts, so that short-period pulsators are labelled $\mathrm{sdBV_r}$ and long-period pulsators $\mathrm{sdBV_s}$ (for *rapid* and *slow*) and pulsators with hybrid behaviour as $\mathrm{sdBV_{rs}}$. However, as we will learn from the data presented here, it may be too early yet to settle this issue, since many more stars than originally anticipated appear to show hybrid behaviour at low amplitudes. This means that we have to face the possibility that all sdBVs are hybrids at some level. For this reason we will stick to using the variable star classes as designators for the dominant pulsational behaviour, and reserve the DW Lyn-type designation for stars that show clear and unambiguous pulsations at both short and long periods, while we refer to stars that are predominantly V361 Hya (or V1093 Her) stars but with low-level pulsations of the other type as being of the predominant type with hybrid behaviour.

Non-adiabatic pulsation calculations show that the V361 Hya stars exhibit low n, low ℓ pressure modes excited by the κ mechanism due to a Z-bump in the envelope (Charpinet et al. 1997), and the V1093 Her stars can be understood in terms of gravity modes of high n excited by the same κ mechanism (Fontaine et al. 2003). The pulsations are facilitated by radiative levitation, which ensures that sufficient iron-group elements are present to cause a Z-bump in the driving region.

Our various surveys have found that only one in 10 sdBs in the hot end of the instability region pulsates with short-period oscillations (Østensen et al. 2010a), while long-period pulsations appear in at least 75 per cent of all stars in the cool end of the instability region (Green et al. 2003), as determined from ground-based observations. The amplitudes for the V1093 Her stars are so low that it has been speculated that most sdB stars cooler than the boundary between the V361 Hya and the V1093 Her stars are pulsators, but with such low amplitudes that they are undetectable without extraordinary efforts from ground-based observatories.

It is an unsolved mystery why so few of the hot stars oscillate. Diffusion calculations have shown that sufficient iron to excite pulsations builds up in the driving region of sdB stars after only 10^6 yr (Fontaine et al. 2006), which is just 1 per cent of the EHB lifetime, implying that ∼99 per cent should pulsate. Most short-period sdBVs that have been monitored regularly over the past decade have shown pulsations with strongly variable amplitudes (Kilkenny 2010). Some pulsation frequencies have even been reported to disappear completely. It is therefore possible that many of the stars that have been surveyed and found not to show variability, may in fact just be passing through an intermittent, quiet phase. With the continuous monitoring provided by *Kepler*, we will be able to quantify both fast and slow pulsations with much lower amplitudes than can be reached from ground-based observations, and determine if pulsation episodes occur.

The *Kepler* spacecraft was launched in March of 2009, with the primary aim to find Earth-size planets using the transit method (Borucki et al. 2010). In order to have a high probability of finding such planets, the spacecraft is designed to continuously monitor the brightness of a massive number of stars with micromagnitude precision. The *Kepler* Field of View (FoV) covers 105 $\mathrm{deg^2}$ in Cygnus and Lyra (about 10–20° from the Galactic plane) using 42 CCDs. As a by-product, high-quality photometric data of pulsating stars in the same field are obtained, an incredibly valuable input for asteroseismology studies (Gilliland et al. 2010a), and a unique opportunity for asteroseismology studies of V1093 Her stars in particular, since adequate observations are nearly impossible to obtain from the ground (Randall et al. 2006).

The first four quarters of the *Kepler Mission* were dedicated to a survey phase, for the asteroseismology subset of targets. A substantial number of target buffers for short-cadence observations have been made available to the *Kepler* Asteroseismic Science Consortium (KASC) during this survey phase. After the survey phase, KASC observations will only be possible on specific targets selected from the survey sample. The primary goal of the survey phase is

[1] Note that this limit is based on temperatures that were derived by fits to metal-free NLTE models. Metal blanketed LTE models such as those used here typically produce effective temperatures that are cooler by 5–10 per cent.

Downloaded from https://academic.oup.com/mnras/article-abstract/409/4/1470/984924 by guest on 29 April 2020

therefore to identify the most interesting pulsators in the sample. These objects can then be followed throughout the remaining years of the mission, with goals including (i) detecting low-amplitude (<100 ppm) and high-degree ($\ell > 2$) modes, normally not visible from the ground; (ii) measuring stellar global parameters with unprecedented accuracy (mass, rotation, envelope thickness and surface gravity); (iii) improving the physical understanding of these stars (differential rotation, core C/O ratio, neutrino cooling and crystallization in the WDs); (iv) studying amplitude variability and non-linear effects; (v) via the O–C diagram, measure the rate of period change, determine the evolutionary status of the star and search for low-mass companions (brown dwarfs or planets, Silvotti et al. 2007) with masses down to $\sim 0.1 M_{\rm J}$.

This paper is the first in a series on compact pulsators in the *Kepler* field, and describes the methods with which the candidates were selected, and provides classifications and noise limits on the targets in the first half of the survey sample. The first analysis of a V361 Hya star in the *Kepler* field are presented by Kawaler et al. (2010a, Paper II), the first results on V1093 Her and DW Lyn pulsators are presented by Reed et al. (2010, Paper III), and a detailed asteroseismic analysis of *Kepler* data on one of these DW Lyn pulsators are given by Van Grootel et al. (2010, Paper IV). Results on two V1093 Her pulsators in sdB+dM reflection binaries are discussed in Kawaler et al. (2010b, Paper V).

2 SURVEY SAMPLE SELECTION

For the survey phase of the *Kepler Mission,* three groups submitted proposals containing candidate hot subdwarf and white dwarf stars. Of the stars included in these proposals, 142 were accepted into the list of KASC survey stars. Of these, six were observed during the 9.7-d commissioning run, and 57 were observed during the first four (out of 10) survey months. All 63 stars are listed in Table 1,

Table 1. Compact pulsator candidates observed with *Kepler*.

KIC	Name	Run	RA (J2000)	Dec. (J2000)	*Kp*	$F_{\rm cont}$	Sample	Class
1868650	KBS 13	Q1	19:26:09.4	+37:20:09	13.45	0.158	a	sdB+dM
2297488	J19208+3741	Q1	19:20:49.9	+37:41:39	17.18	0.833	c	sdO+F/G
2692915	J19033+3755	Q2.3	19:03:22.7	+37:55:30	17.54	0.758	d	DO
2697388	J19091+3756	Q2.3	19:09:07.1	+37:56:14	15.39	0.149	cf	sdBV
2991276	J19271+3810	Q2.1	19:27:09.1	+38:10:26	17.42	0.971	c	sdB
2991403	J19272+3808	Q1	19:27:15.9	+38:08:08	17.14	0.601	c	sdBV+dM
3427482	J19053+3831	Q1	19:05:22.5	+38:31:33	17.31	0.891	c	DA
3527617	J19034+3841	Q2.2	19:03:24.9	+38:41:24	17.54	0.554	c	He-sdOB
3527751	J19036+3836	Q2.3	19:03:37.0	+38:36:13	14.86	0.081	cf	sdBV
3729024	J19014+3852	Q2.2	19:01:25.8	+38:52:33	17.63	0.611	c	sdB
4244427	J19032+3923	Q2.1	19:03:17.6	+39:23:14	17.35	0.781	c	sdB
4829241	J19194+3958	Q1	19:19:27.7	+39:58:39	15.83	0.435	e†	DA
5342213	J18568+4032	Q2.2	18:56:49.5	+40:32:51	17.68	0.362	c	sdOB
5775128	2M1905+4101	Q2.3	19:05:01.0	+41:01:53	13.54	0.023	bf	B
5807616	KPD 1943+4058	Q2.3	19:45:25.5	+41:05:34	15.02	0.332	a	sdBV
5942605	FBS 1858+411	Q2.1	19:00:27.8	+41:15:04	14.08	0.088	a	B
6188286	J19028+4134	Q2.3	19:02:49.9	+41:34:58	14.21	0.028	f	sdOB
6669882	J18557+4207	Q2.3	18:55:46.0	+42:07:04	17.94	0.468	d	DA
6848529	BD +42°3250	Q0	19:07:40.5	+42:18:22	10.73	0.003	a‡	sdB
6862653	J19267+4219	Q2.3	19:26:46.0	+42:19:34	18.19	...	d	DB
7353409	2M1915+4256	Q2.2	19:15:18.9	+42:56:13	14.68	0.091	b	sdO
7434250	J19135+4302	Q2.3	19:13:35.6	+43:02:56	15.47	0.287	d	sdB
7664467	J18561+4319	Q2.3	18:56:07.1	+43:19:19	16.45	0.879	f	sdBV
7755741	2M1931+4324	Q1	19:31:08.9	+43:24:58	13.75	0.112	b	sdO
7975824	KPD 1946+4340	Q1	19:47:42.9	+43:47:31	14.65	0.106	a‡	sdOB+WD
8022110	J19179+4350	Q2.3	19:17:58.7	+43:50:21	16.55	0.316	f	sdB
8077281	J18502+4358	Q2.3	18:50:16.9	+43:58:28	16.57	0.296	f†	B
8142623	J18427+4404	Q1	18:42:42.4	+44:04:05	17.30	0.388	de†	sdB
8496196	J19288+4430	Q2.3	19:28:51.1	+44:30:13	16.45	0.827	f	sdOB
8619526	J19195+4445	Q1	19:19:30.5	+44:45:43	15.84	0.256	f†	PNN
8682822	J19173+4452	Q1	19:17:20.6	+44:52:40	15.81	0.473	e†	DA
8751494	J19241+4459	Q2.2	19:24:10.8	+44:59:35	16.27	0.566	e†	CV
8889318	J19328+4510	Q2.3	19:32:50.6	+45:10:23	17.17	0.645	d	sdB
9139775	J18577+4532	Q2.3	18:57:43.6	+45:32:19	17.92	0.272	d	DA
9202990	J18561+4537	Q2.3	18:56:08.0	+45:37:40	15.04	0.119	d‡	CV
9408967	J19352+4555	Q2.3	19:35:12.2	+45:55:42	17.26	0.807	d	He-sdOB
9472174	2M1938+4603	Q0	19:38:32.6	+46:03:59	12.26	0.022	b	sdBV+dM
9543660	2M1951+4607	Q1	19:51:56.2	+46:07:51	13.77	0.459	b	sdOB
9569458	J18477+4616	Q1	18:47:43.6	+46:16:26	17.18	0.031	d	sdB
9583158	NSV 11917	Q2.1	19:19:10.2	+46:14:51	17.32	0.465	ad	PNN
9822180	J19100+4640	Q2.1	19:10:00.3	+46:40:25	14.58	0.215	d	sdO+F/G
9957741	J19380+4649	Q2.1	19:38:01.6	+46:49:45	16.10	0.099	f	He-sdOB
10130954	2M1910+4709	Q0	19:10:23.7	+47:09:44	11.13	0.001	bf	B

Downloaded from https://academic.oup.com/mnras/article-abstract/409/4/1470/984924 by guest on 29 April 2020

Table 1 – *continued*

KIC	Name	Run	RA (J2000)	Dec. (J2000)	*Kp*	$F_{\rm cont}$	Sample	Class
10139564	J19249+4707	Q2.1	19:24:58.2	+47:07:54	16.13	0.608	f	sdBV
10220209	2M1945+4714	Q2.3	19:45:33.2	+47:14:17	14.12	0.090	bf	B
10285114	2M1944+4721	Q0	19:44:02.7	+47:21:17	11.23	0.028	bf	B
10420021	J19492+4734	Q2.2	19:49:14.6	+47:34:46	16.20	0.909	e	DA
10482860	J19458+4739	Q2.3	19:41:34.2	+49:07:14	17.80	0.640	d	DO
10593239	J19162+4749	Q2.3	19:16:12.2	+47:49:16	15.28	0.120	d	sdB+F/G
10658302	2M1915+4754	Q2.1	19:15:07.9	+47:54:20	13.12	0.148	bf	B
10661778	J19211+4759	Q2.3	19:21:11.1	+47:59:24	17.66	0.483	d	sdB
10670103	J19346+4758	Q2.3	19:34:39.9	+47:58:12	16.53	0.450	f	sdBV
10982905	J19405+4827	Q2.1	19:40:32.2	+48:27:24	14.15	0.154	d	sdB+F/G
11032470	J19327+4834	Q2.2	19:32:45.3	+48:34:47	16.13	0.680	f	F
11179657	J19023+4850	Q2.3	19:02:21.9	+48:50:52	17.06	0.129	d	sdBV+dM
11357853	J19415+4907	Q2.1	19:41:34.3	+49:07:14	17.37	0.632	d	sdOB
11454304	2M1925+4918	Q0	19:25:24.4	+49:18:56	12.95	0.007	bf	B
11514682	J19412+4925	Q2.3	19:41:12.4	+49:25:06	15.69	0.436	d	DAB
11717464	J19369+4953	Q1	19:36:55.8	+49:53:14	15.73	0.525	f	A
11817929	2M1935+5002	Q0	19:35:38.4	+50:02:35	10.38	0.002	bf	B
11822535	WD 1942+499	Q2.2	19:43:41.8	+50:05:01	14.82	0.155	a	DA
11953267	2M1901+5023	Q2.2	19:01:35.2	+50:23:06	13.50	0.071	bf	B
12156549	J19193+5044	Q2.3	19:19:18.8	+50:44:04	15.89	0.107	d	DA+dMe

Notes. *Kp* is the magnitude in the *Kepler* bandpass, $F_{\rm cont}$ is the contamination factor from the KIC. The samples are: a: Literature, b: 2MASS, c: SDSS, d: *Galex,* e: RPM, f: KIC colour. † and ‡ mark targets with TNG and NOT photometry, respectively.

where we also give a name for each target from the literature, or an abbreviated coordinate designation. The survey month, target coordinates, *Kepler magnitude* (*Kp*),[2] estimated contamination factor ($F_{\rm cont}$), original survey sample and our final classification (see Section 3) are also listed in the table. Note that the large FoV of *Kepler* implies that the resolution is only around 4 arcsec per pixel (see Bryson et al. 2010). Typically, for our faint targets, 4–10 pixels are summed to capture all the flux, with the number increasing for targets located towards the edges of the field. Contamination from nearby stars can be severe, as indicated by the sometimes large $F_{\rm cont}$ values in Table 1. Survey months for the *Kepler Mission* are referred to in the following way: Q0 refers to the commissioning period; Q1 refers to the first 33.5-d survey cycle (2009 May 12–June 14); Q2 refers to the second quarter of the survey phase (90 d), subdivided into three monthly cycles. All objects are referred to by their identifier from the *Kepler* Input Catalogue (KIC), but we will refer to many of the stars listed here by their name from the survey that first identified them as compact stars. For convenience, both names are listed in the tables in this paper. For the stars from the SDSS and *Galex* surveys, we have used abbreviated coordinate names throughout our spectroscopic survey, and these are retained in the tables and discussions here. When we start discussing the photometric properties of these targets, we will prefer the KIC identifiers, in order to conform with other works on *Kepler* photometry. Note that even if the table is sorted by KIC identifiers, it is easy to locate an object by coordinate name, since KIC numbers are allocated in order of increasing declination.

The different methods used to construct this sample are summarized in the following sections.

[2] The *Kp* magnitudes approximates the passband of the *Kepler* photometer and is computed from *B* and *V* magnitudes from the Tycho-2 catalogue. For blue stars the formula is $Kp = 0.344B + 0.656V - 0.032$.

2.1 Known compact stars from the literature

A few subdwarfs from earlier blue-star surveys were already known to be located within the *Kepler* FoV. The bright sdB star BD +42°3250 ($B = 10.4$) was known not to pulsate from the study of Østensen et al. (2010a), but included in the survey anyway since its brightness permits by far the highest S/N ratio of the stars in the sample, potentially revealing the presence of extremely low level pulsations. KPD 1946+4340 and KPD 1943+4058 were reported to be hot subdwarf stars in the Kitt Peak Downes survey (Downes 1986). KPD 1946+4340 was also known to be a binary system with a period of 0.4 d from the radial velocity survey of Morales-Rueda et al. (2003). It was also included in the variability survey of Østensen et al. (2010a), but was not found to vary on short time-scales above the millimagnitude level.

Also, the *First Byurakan Survey* for blue stellar objects (FBS, Abrahamian et al. 1990) contains a few fields that overlap with the *Kepler* FoV. Three stars from the FBS were identified as likely sdB stars, but none of them has been studied in detail up to now. The star KBS 13 was identified in the first *Kepler* Blue Star (KBS) survey, and identified as a reflection effect sdB+dM binary by For et al. (2008).

Two white dwarf stars in the *Kepler* field were also known from the literature. WD 1942+499 is a DA white dwarf, but with a temperature of 33 500 K (Marsh et al. 1997) it is far too hot to reside in the ZZ Ceti instability region. NSV 11917 is the planetary nebula nucleus (PNN) of Abell 61 (Abell 1966), and its temperature was estimated to be ∼88 000 K by Napiwotzki (1999).

2.2 The 2MASS sample

A list of 171 candidates was obtained from the 2MASS catalogue (Skrutskie et al. 2006) with $J < 15.5$, and colours covering the range of hot subdwarfs, $J - H < 0.01$, $J - K < 0.01$, that were within the FoV of the *Kepler* CCDs and more than five pixels from the edges.

Downloaded from https://academic.oup.com/mnras/article-abstract/409/4/1470/984924 by guest on 29 April 2020

They were then observed spectroscopically with the Bok telescope on Kitt Peak. Unfortunately, of all the targets only two new sdB stars and two new sdO stars were found. Detecting compact stars from 2MASS colours has produced much higher success rates in high Galactic latitude surveys, but since the *Kepler* field is located relatively close to the Galactic plane the contamination of main-sequence B stars is very high down to the limiting magnitude of the 2MASS survey.

Also, one of the stars classified as sdB in the FBS survey appeared in this sample, but the spectroscopy revealed that it was actually another main sequence B star. Pre-launch ground-based photometry of the four hot subdwarfs revealed that one of them (2M1938+4603) has a strong reflection effect with grazing eclipses indicating the presence of a close M-dwarf companion (Østensen et al. 2010b).

2.3 The *Galex* sample

In order to avoid the contamination of hot main-sequence stars, we searched the available archives for ultraviolet (UV) photometry. A reliable photometric characteristic of both hot subdwarfs and white dwarfs is the strong UV-excess relative to normal stars. The UV photometry from the *Galex* satellite (Martin et al. 2005) covers large patches of the northern half of the *Kepler* field, and Guest Observer (GO) fields cover further patches across the field. In total we identified 27 UV-excess targets from the *Galex* GR4 catalogue, and a further 24 from guest observer fields kindly made available to us. As expected, selecting targets based on UV photometry turned out to be extremely successful. Of the 20 stars in the current sample that were selected from *Galex* photometry, all are hot subdwarfs or white dwarfs.

2.4 The SDSS/SEGUE sample

The SEGUE extension (Yanny et al. 2009) of the Sloan Digital Sky Survey (SDSS, Stoughton et al. 2002) contains a single stripe that crosses the south-western part of the *Kepler* target field. Searching the Sloan data base for UV-excess targets revealed 19 acceptable targets brighter than $g = 17.5$. Of these, three have spectroscopy in SDSS/SEGUE identifying them as hot subdwarfs. But selecting on the near-optical u colour is as effective in distinguishing compact stars from normal stars as using *Galex* far-UV colours; all 10 stars selected from the current sample with this method turned out to be hot subdwarfs or white dwarfs.

2.5 The reduced proper motion sample

19 candidates were selected using the reduced proper motion (RPM) method, which is a powerful tool to identify white dwarfs in photometric surveys. RPM is defined as $(Kp + 5\log\mu + 5)$, where μ is the proper motion in arcsec yr^{-1} from the USNO catalogue. When plotted against the $g - i$ colour from the KIC, hot high proper motion objects are easily isolated (see Fig. 1). However, the $g - i$ colour is not a precise temperature indicator and therefore it is difficult to say whether these targets fall inside one of the known instability strips. On the other hand, unknown instability strips might exist as shown by recent discoveries: the first (and up to now unique) sdO pulsator (Woudt et al. 2006) and the first hot DQ oscillating white dwarf (Montgomery et al. 2008).

For hot subdwarfs the method has a lower likelihood of producing successful results, since these stars are typically much more distant than white dwarfs, and the USNO proper motions are not precise enough to be useful in most cases. Five of the 19 candidates are included in the current survey sample, and our spectroscopy has confirmed that four of them are indeed white dwarfs, and the remaining one is an sdB star.

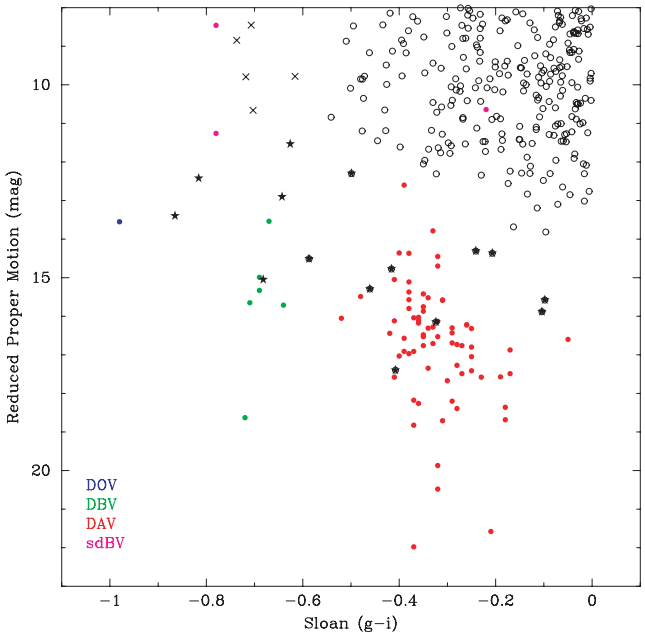

Figure 1. The reduced proper motion diagram used to select targets from the KIC. Blue, red, green and magenta symbols are known pulsators from the literature, while black points mark KIC entries (stars: WD candidates, crosses: sdB candidates, circles: other). Note that while single sdB stars are exceedingly blue, sdB stars with F-/G-/K-star companions overlap with the general population of blue stars.

2.6 Targets selected on KIC colours

The KIC contains $g - r$ colours that can be used to select blue stars. However, without a UV colour it is not really possible to distinguish between normal B stars and hot subdwarfs, in particular because one-third of sdBs are found in binary systems with F–K companions, and are therefore redder than they would be as single stars. However, since B stars are much more luminous than subdwarfs and white dwarfs, below a magnitude of around ∼15, the limited thickness of the Galactic disc ensures that any blue star is much more likely to be a compact object than a main-sequence or regular horizontal branch star.

Two of the proposals used this strategy for the bulk of their targets, and unfortunately only one of those had access to the results of the 2MASS survey. Thus, eight stars known to be normal B stars entered the current sample. However, of the remaining 13 stars selected with this method, 10 turned out to be compact objects from our spectroscopy.

3 GROUND-BASED OBSERVATIONS

Throughout the period leading up to the release of the first *Kepler* data we undertook preliminary ground-based photometry and spectroscopy of most of the targets in the *Kepler* sample, in order to improve the classifications from the initial surveys.

Downloaded from https://academic.oup.com/mnras/article-abstract/409/4/1470/984924 by guest on 29 April 2020

Table 2. Log of spectroscopic observations.

Date	Tel-run	N_t	PI + Observer(s)
2008 June–September	Bok	15	EMG
2008 August 16	INT-1	2	CRL, MV
2008 September 20–24	NOT-1	19	RO
2009 April 11–12	WHT-1	37	CA, RHØ
2009 June 5–10	INT-2	2	RO, RHØ, TAO
2009 July 14–16	WHT-2	32	CA, TAO
2009 August 14	NOT-2	2	JHT, TL
2009 September 7	NOT-3	5	JHT

Note.—N_t lists the number of targets observed during the run that actually entered the *Kepler* compact star survey sample.

3.1 Spectroscopy

We obtained classification spectra of all the targets in Table 1 using low-resolution spectroscopy at various telescopes, as listed in Table 2.

The observations at the Isaac Newton Telescope (INT) used the IDS spectrograph with the 235-mm camera and the R400B grating, providing a resolution of $R \approx 1400$ and an effective wavelength coverage $\lambda = 3020$–6650 Å. At the Nordic Optical Telescope (NOT) we used the ALFOSC spectrograph, with grism #6 in 2008, and grism #14 in 2009. Both give $R \approx 600$ for the wide slit we used, and $\lambda = 3300$–6200. On the William Herschel Telescope (WHT) we used the ISIS spectrograph with grating R300B on the blue arm ($R \approx 1600$, $\lambda = 3100$–5300 Å). Red-arm spectra were also obtained, but have not been used for this work. Observations from the Bok telescope on Kitt Peak were done with the B&C spectrograph using a 400 mm^{-1} grating ($R \approx 550$, $\lambda = 3620$–6900 Å).

All data were reduced with the standard IRAF procedures for long-slit spectra. The bias levels were estimated from the overscan region of each image, and a large number of flat-field images were averaged in order to calibrate the pixel-to-pixel response. Arc reference spectra were taken frequently during the observations, and each target spectrum was wavelength calibrated with the closest available arc. For some of the observation runs no radial velocity (RV) or flux standards were obtained, as the purpose of the observations was to produce classification spectra that do not require such detailed calibration.

3.1.1 *Spectral classification*

All stars were classified spectroscopically to distinguish the compact pulsator candidates from contaminating objects. In the sample of 63 stars, only 12 were found to have spectra indicating that they are main-sequence or horizontal branch stars (the classifications are given in Table 1). It is worth noting that almost all of the main-sequence B stars that contaminate our sample are variable, although with much longer periods than would be exhibited by our compact objects. However, we will not discuss these stars further in this paper.

Three unusual objects are worth particular mention, and we show their spectra in Fig. 2. The slopes of these spectra were rectified from the instrumental response to a normalized flux scale by dividing the spectrum with a response function computed by calibrating an extinction-corrected spectrum of a single sdB star against a flux model spectrum for its atmospheric parameters.

J18561+4537 shows Balmer line cores apparently filled in by emission, and J19241+4459 shows Balmer lines in clear emission, and we classify both objects as cataclysmic variable (CV) systems.

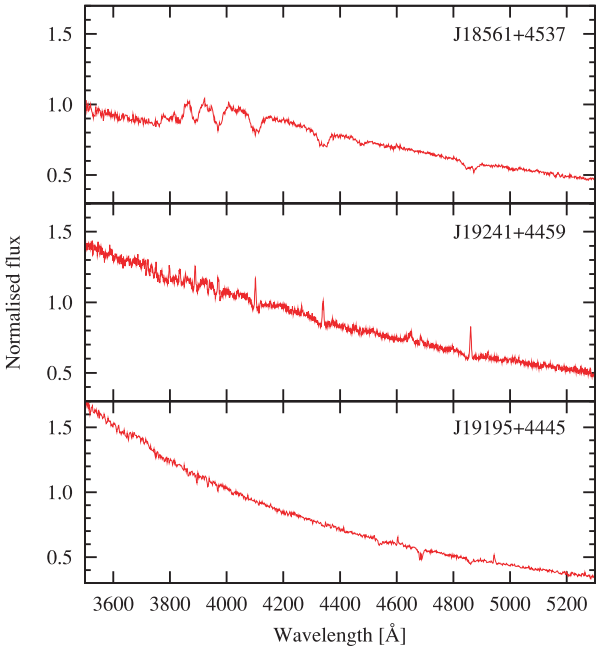

Figure 2. Spectra of two cataclysmic variables and one planetary nebula nucleus (bottom).

They are both strongly variable in the *Kepler* photometry, and we give a brief description of these objects in Section 4.7.

J19195+4445 is an extraordinary hot object. Very few features are visible in its hot continuum, but the combination of C IV and He II close to 4686 Å is a hallmark of the PG1159 stars. Kronberger et al. (2006) have noted a 'possible bipolar PN' which they call DSH J1919.5+4445, with an area of about 2 arcmin centred roughly on the coordinates of our object. We conclude that J19195+4445 is the central star of that nebula.

3.1.2 *Properties of the hot subdwarfs*

We have determined the physical parameters of all the sdB stars in our sample, except for two that are strongly contaminated by a companion (listed as sdB+F/G in Table 1). The physical parameters derived from our model fits are listed in the last columns of Tables 3 and 4. Almost all the sdB stars show the Ca II *H* and *K* lines characteristic of sdBs with main-sequence F/G/K companions, but in our low-resolution spectra it is not possible to distinguish the Ca II signature of a main-sequence companion from interstellar absorption, which can be quite substantial at the relatively low Galactic latitudes of the *Kepler* field. Only J19162+4749 and J19405+4827 are clearly composite-spectrum sdB plus F or G binaries, and we refrain from attempting to determine physical parameters for these two stars due to the strong contamination. One star, J19415+4907, was classified as sdOB based on the presence of both He I and He II lines in its spectrum, but we failed to obtain a satisfactory solution in the model-fitting procedure. The object appears to be hotter than 40 000 K, but a higher S/N spectrum would be required to make firm conclusions.

The effective temperature ($T_{\rm eff}$), surface gravity ($\log g$) and photospheric helium abundance [$\log y = \log (N_{\rm He}/N_{\rm H})$] were derived by fitting model atmosphere grids to the hydrogen and helium lines visible in the spectra, which in all cases include Balmer lines up to H_{13}. The fitting procedure used here was the same as that of Edelmann et al. (2003), but we used only the metal-line

Downloaded from https://academic.oup.com/mnras/article-abstract/409/4/1470/984924 by guest on 29 April 2020

Table 3. Properties of sdB stars with no significant pulsations.

		100–500 μHz			500–2000 μHz			2000–8488 μHz			Spectroscopic data			
KIC	Name	σ (ppm)	A_+ σ	f_+ (μHz)	σ (ppm)	A_+ σ	f_+ (μHz)	σ (ppm)	A_+ σ	f_+ (μHz)	$T_{\rm eff}$ (kK)	$\log g$ (dex)	$\log y$ (dex)	Tel-run
9569458	J18477+4616	92	4.0	195	91	3.5	881	92	3.7	5516	27.8(2)	5.34(3)	–2.7(1)	WHT-2
4244427	J19032+3923	97	3.5	245	95	4.1	1253	95	4.0	2903	28.1(2)	5.55(3)	–2.0(1)	WHT-2
8022110	J19179+4350	42	2.9	146	41	3.5	1322	41	3.5	6324	28.9(2)	5.50(3)	–2.6(1)	WHT-2
6848529	BD +42°3250	3	2.8	473	2	3.3	1880	2	3.8	4887	28.7(1)	5.08(2)	–1.6(1)	WHT-1
											29.5(1)	5.13(2)	–1.5(1)	Bok
10661778	J19211+4759	99	3.5	452	97	3.5	805	98	4.1	2914	29.4(2)	5.56(4)	–2.8(1)	WHT-2
1868650	KBS 13	7	3.4	297	7	3.6	1365	7	3.7	5033	29.7(1)	5.70(1)	–1.7(1)	Bok
3729024	J19014+3852	137	3.1	200	133	3.5	693	134	3.8	2587	30.6(7)	5.83(9)	–3.2(1)	SDSS
6188286	J19028+4134	10	4.0	188	10	4.1	1206	10	3.9	4921	31.6(2)	5.81(2)	–1.7(1)	WHT-1
7434250	J19135+4302	20	4.0	183	19	3.4	576	19	3.9	6196	32.0(4)	5.17(7)	–2.8(2)	WHT-1
8889318	J19328+4510	62	3.4	412	61	3.7	1614	62	3.8	3843	32.4(5)	5.67(9)	–2.4(4)	WHT-1
8142623	J18427+4404	118	3.0	274	115	3.7	653	116	4.0	4291	34.1(2)	5.65(3)	–1.5(1)	WHT-2
7975824	KPD 1946+4340	9	3.2	275	9	3.7	1156	9	4.1	5018	34.3(3)	5.20(12)	–1.3(1)	
5342213	J18568+4032	157	3.6	182	155	3.3	1620	156	3.6	4033	35.7(2)	5.78(5)	–1.5(1)	WHT-2
8496196	J19288+4430	41	3.1	323	41	3.7	1189	40	3.9	8065	36.1(2)	5.85(4)	–1.6(1)	WHT-2
9543660	2M1951+4607	7	3.4	221	7	3.6	1994	7	4.0	3826	37.7(1)	5.66(2)	–2.3(1)	Bok
10593239	J19162+4749	Var. comp.			18	3.3	576	18	3.7	5732	Strong composite			NOT-1
10982905	J19405+4827	9	3.3	314	8	3.5	1098	8	3.7	4797	Strong composite			NOT-1

Table 4. Properties of the sdBV stars.

		Kepler data					Spectroscopic data			
KIC	Name	N_f	$f_{\rm med}$ (μHz)	$f_{\rm min}$ (μHz)	$f_{\rm max}$ (μHz)	$P_{\rm orb}$ (d)	$T_{\rm eff}$ (kK)	$\log g$ (dex)	$\log y$ (dex)	Tel-run
10670103	J19346+4758	28	131.6	61.4	203.2	...	20.9(3)	5.11(4)	–2.2(3)	NOT-3
2697388	J19091+3756	37	183.1	89.1	3805.9	...	23.9(3)	5.32(3)	–2.9(1)	NOT-1
11179657	J19023+4850	11	271.5	186.5	351.6	0.394	26.0(8)	5.14(13)	–2.1(2)	WHT-1
7664467	J18561+4319	6	207.5	110.2	246.9	...	26.8(5)	5.17(8)	–2.8(2)	WHT-2
5807616	KPD 1943+4058	21	224.1	109.5	3447.2	...	27.1(2)	5.51(2)	–2.9(1)	Bok
2991403	J19272+3808	7	283.7	194.7	334.8	0.443	27.3(2)	5.43(3)	–2.6(1)	WHT-2
3527751	J19036+3836	41	275.1	92.1	3703.3	...	27.6(2)	5.28(3)	–2.9(1)	NOT-1
							28.2(3)	5.46(5)	–2.9(1)	INT-1
							27.9(2)	5.37(9)	–2.9(1)	(Adopted)
9472174	2M1938+4603	>55	2065.9	50.3	4531.6	0.126	29.6(1)	5.42(1)	–2.4(1)	Bok
10139564	J19249+4707	20	5709.4	316.0	7633.6	...	32.5(2)	5.81(4)	–2.3(1)	WHT-2
2991276	J19271+3810	1	8201.1			...	33.9(2)	5.82(4)	–3.1(1)	WHT-2

blanketed LTE models of solar composition described in Heber, Reid & Werner (2000). Note that for the hottest stars in the sample, NLTE effects start to become significant (Napiwotzki 1997), and that the LTE models can underestimate the temperatures by up to 1000 K in some cases. It is also known that sdB stars have very peculiar abundance patterns. In general the light elements (He to S) are deficient with respect to the Sun (Edelmann, Heber & Napiwotzki 2006), while some iron-group and even heavier elements (e.g. lead) can be strongly enriched (O'Toole & Heber 2006; Blanchette et al. 2008). The iron abundance, however, is found to be nearly solar (with a scatter ±0.5 dex from star to star) in a sample of 139 sdB stars, irrespective of the effective temperature (Geier et al. 2010). Therefore, we decided to use model atmospheres of solar metal content, which account for metal-line blanketing through opacity distribution functions, for the quantitative spectral analysis (Heber et al. 2000). The helium abundance is determined for each star individually. The peculiar metal abundance patterns are, hence, unaccounted for and might introduce some uncertainties when determining $T_{\rm eff}$ and $\log g$. The errors given on the last digit in Tables 3 and 4 only reflect the formal errors when fitting the models to the observed spectra. Systematics when using grids with different numerical approximations or metallicities can be much more significant than the formal errors, especially for the stars with high S/N spectra, which appear with extremely low error bars in Fig. 3.

The parameters of the pulsators are given in Table 4, together with their variability data. Remarkably, all the stars in our sample which converge to temperatures below ∼27 500 K on our LTE grid appear to be pulsators (see Fig. 3). Several stars lie in the region close to 28 000 K where the hybrid DW Lyn-type pulsators are found. Three of the long-period pulsators also show signs of pulsation periods with frequencies short enough to be *p*-modes, although with extremely low amplitudes.

3.2 Photometric observations

Prior to the *Kepler* launch, ground-based preliminary observations were done for 27 targets, including all those with known proper motion. Time series photometry on 24 of these was performed at

Downloaded from https://academic.oup.com/mnras/article-abstract/409/4/1470/984924 by guest on 29 April 2020

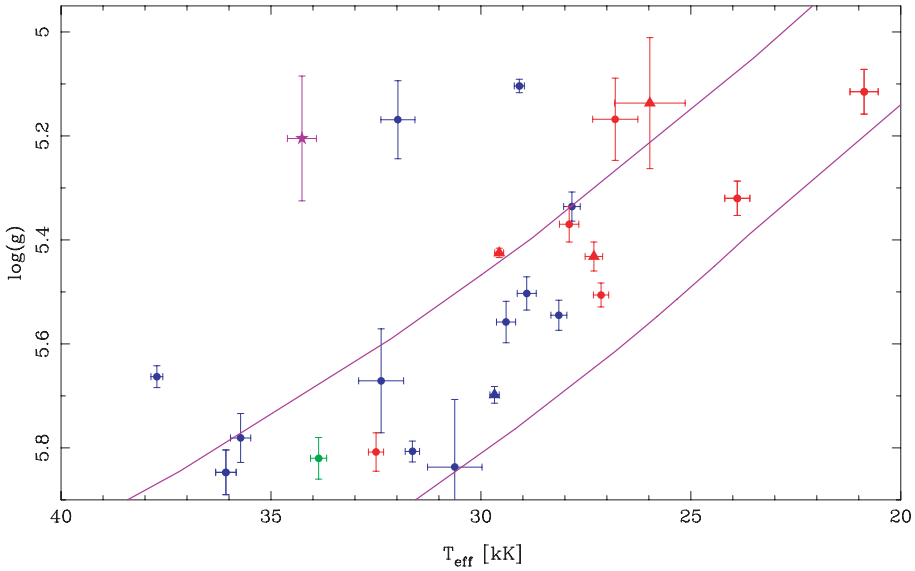

Figure 3. The $T_{\rm eff}$/log g plane for the sdB stars in our sample. Red symbols indicate the pulsators, blue symbols the non-pulsators, with the transient pulsator marked with a green symbol. The sdB+dM reflection binaries are marked with triangles, and the eclipsing sdB+WD system (which is also a candidate pulsator) is marked with a star.

the 3.6-m Telescopio Nazionale Galileo (TNG) in August of 2008 using the DOLORES camera (marked with a † in Table 1). Each target was observed once for 1–2 h with the g filter, and exposure times between 1 and 10 s, depending on the magnitude. The data were reduced using standard techniques (see e.g. Silvotti et al. 2006), using typically seven comparison stars (minimum four). A preliminary analysis of these data did not show any clear signature of intrinsic pulsation in any of the stars observed (Silvotti et al. 2009) and the typical upper limits to the pulsation amplitude were between 0.1 and 0.2 per cent. However, for two sdB candidates a low amplitude variability was suspected: a peak at 125 s with an amplitude of about 0.1 per cent at 3.5 times the noise level was found in KIC2020175 (= J19308+3728, a Q3.1 *Kepler* target) and a possible period of about 1 h with an amplitude of ∼0.4 per cent was detected in KPD 1943+4058. Indeed, *Kepler* has confirmed that KPD 1943+4058 is a g-mode pulsator (see Table 4 and Section 4.4 below). Moreover, the TNG data revealed high amplitude (∼10 per cent) variability for the CV J19241+4459 (see Section 4.7 below), and ground-based follow-up photometry and spectroscopy have recently been published by Williams et al. (2010).

Another three targets were observed with NOT/ALFOSC in fast photometry mode (marked with a ‡ in Table 1). Two showed no particular features, and the photometric limits were included in the study of Østensen et al. (2010a), and one star observed during the NOT-1 run was found to show substantial photometric activity on longer time-scales, but the 1-h run was too short to make any further conclusions. The *Kepler* photometry clearly reveals this object, J18561+4537 (KIC9202990) to be a cataclysmic variable (see Section 4.7, below).

4 *KEPLER* OBSERVATIONS

Both sdBs and WDs are rare objects in the field. The large PG and KPD surveys detected only about five sdBs with $B < 16$ per 100 deg^{-2} of sky, and half of that for the WDs. The FoV of *Kepler* covers about that area, so in order to have a reasonable chance of finding a pulsator, it was necessary to extend the limit to a magnitude of ∼17.5. The high photometric accuracy of *Kepler* ensures that we can still detect pulsators at this magnitude, and therefore that compact pulsators remain viable targets for the mission. Although the 1-min cadence is not ideal for the short periods often found in these targets, it is short enough to detect most if not all the pulsation periods of these stars, which are typically between about 2 min and 2 h.

4.1 Sample statistics

Our initial statistics predicted about 12 sdBV (four short-period and eight long-period sdBVs) and 2–3 ZZ Ceti pulsators within the 17.5 mag limit. The DBV and GW Vir stars are more rare, and would only be found by a stroke of luck. These numbers were obtained assuming a local space density of 1.2×10^{-4} pc^{-3} (ZZ Ceti), 4×10^{-8} pc^{-3} (V361 Hya) and 8×10^{-8} pc^{-3} (V1093 Her), a disc scaleheight of 500 pc, and considering a fraction of pulsators within each instability strip of 1, 0.1 and 0.5, respectively (see Silvotti 2004, for more details). Note that, due to their intrinsic faintness, all the DAVs observable with *Kepler* belong to the Galactic disc, implying that their number is highly dependent on the magnitude limit (while this is only marginally true for the sdBs). The number of DAVs potentially observable with *Kepler* increases by a factor of ∼4 when increasing the magnitude limit by one unit.

The initial statistics have now been confirmed to a large extent by our spectroscopic observations, as our efforts have securely identified 70 hot subdwarfs down to a magnitude of 17.7. As many as 56 of these are sdBs and sdOBs (exactly the number expected from the space densities and pulsator fractions stated above), seven are He-sdOBs, and seven are sdOs, although the exact number of pulsators remains to be determined as only half of the photometric survey data have been released. For the WDs the numbers are about as expected; 15 DAs, two DBs, one DO, two PNNi and two CVs. About half of these targets are listed in Table 1, the remainder will be described following the release of the second half of the survey phase of the mission.

Downloaded from https://academic.oup.com/mnras/article-abstract/409/4/1470/984924 by guest on 29 April 2020

4.2 The *Kepler* photometry

Kepler short-cadence (SC) photometry consists of light curves with 58.8-s sampling, each around 1 month in length, except for the shorter Q0 commissioning cycle which only included relatively bright objects. The light curves from Q0 and Q1 are virtually uninterrupted, but in Q2 events on July 2 triggered a processor reset that caused the spacecraft to enter safe mode. Such safing events produce gaps in the light curves, and the July 2 event caused a 2-d gap in time series from Q2.1. Two other minor events caused a loss of fine pointing control, which produced a half-day gap in the photometry from Q2.2, and a 1-d gap in Q2.3. Pointing corrections that did not leave significant gaps also produced minor excursions in the light curves. Such corrections have minimal effect on uncontaminated light curves, but can cause quite significant excursions in the light curves of stars with substantial contamination factors (see Table 1). We fitted first- or second-order polynomials with an exponential decay component to each segment of the light curve and subtracted this function before restoring it back to its mean value. The amplitudes provided in this paper are therefore not corrected for the contamination from close companions. We are concerned that the contamination corrections provided by the KIC are not sufficiently accurate for our targets, as they have spectra that deviate substantially from normal stars, particularly at short wavelengths. A full contamination correction will be performed later for the most important targets, when we have spectroscopic information also on the surrounding stars.

The *Kepler* instrument has an intrinsic exposure cycle consisting of 6.02-s integration followed by a 0.52-s readout period. The SC photometry is a sum of nine such integrations, and long-cadence (LC) photometry are a sum of 270 (Gilliland et al. 2010b). For unknown reasons, the LC cycle produces artefacts in the SC light curve, not just at the LC frequency, $f_{\rm lc} = 566.391\,\mu$Hz, but at all harmonics of this frequency up to the Nyquist frequency, which is $f_{\rm Nyq} = 15 f_{\rm lc} = 0.5 f_{\rm sc} = 8496.356\,\mu$Hz. In most short-cadence light curves, these artefacts get stronger at higher frequencies, typically peaking at $9 f_{\rm lc} = 5098\,\mu$Hz. After the safing event in Q2.1, $f_{\rm lc}$ returned with a different phase, which makes it split up in two peaks of roughly equal amplitude when taking the FT of the full data set, while stellar pulsation peaks remain single-peaked. In these cases it affects a region of the FT up to 2-μHz wide around each multiple of $f_{\rm lc}$, while for all other runs the regions affected are ∼1-μHz wide. Another likely artefact is found at 7865 μHz. It is seen in the light curves of KIC8022110, and 2991276, in the pulsators KIC2697388, 3527751, 10139564, and in the DB white dwarf KIC6862653. KIC2991276 was observed in Q2.1, and the 7865-μHz peak is double just as the $f_{\rm lc}$ artefacts. It thus appears most likely that this peak is instrumental in origin, but its particular cause is not yet known.

4.3 Detections and non-detections

Unambiguous pulsations were detected in nine of the stars classified as hot subdwarf stars in Table 1, and in none of the white dwarfs. For this reason we will concentrate mostly on the subdwarf B stars in this paper, and leave a detailed treatment of the white dwarfs until the survey is complete. After detrending the light curves, we computed their Fourier transforms (FTs) and examined them for pulsations and binary signatures. The pulsators are discussed in Section 4.4, and the binaries in Section 4.6, below.

Tables 3 and 5 list the limits from the *Kepler* photometry, in three different frequency ranges, for all the stars where no clear pulsations were found. We give the arithmetic mean of the amplitude spectrum in the frequency range considered (which for a photon noise dominated signal can be considered as the variance, σ), and the amplitude, A_+, and frequency, f_+, of the highest peak, where A_+ is given as the ratio of the peak amplitude and the σ level.

With only a few exceptions, the frequency analysis of the three frequency regions yields identical results in terms of noise level, which is an evidence of the excellent quality of the *Kepler* photometry. The noise level is found to be ∼8 ppm for $Kp = 14$ and

Table 5. Photometric limits on the non-sdB stars.

		100–500 μHz			500–2000 μHz			2000–8488 μHz			
KIC	Name	σ (ppm)	A_+ (σ)	f_+ (μHz)	σ (ppm)	A_+ (σ)	f_+ (μHz)	σ (ppm)	A_+ (σ)	f_+ (μHz)	Class
2297488	J19208+3741	78	3.5	186.8	76	3.4	1714.8	77	3.8	5174.3	sdO+F/G
2692915	J19033+3755	117	3.2	260.5	112	3.5	1492.1	111	3.7	8249.5	DO
3427482	J19053+3831	92	3.2	465.8	93	3.5	1430.4	94	3.6	3874.2	DA
3527617	J19034+3841	117	3.1	389.9	116	3.5	1383.7	117	3.7	4951.6	He-sdOB
4829241	J19194+3958	22	3.2	421.9	22	3.9	1900.9	22	3.9	8302.4	DA
6669882	J18557+4207	163	3.1	172.9	161	3.4	1316.1	160	3.6	6392.6	DA
6862653	J19267+4219	87	3.7	377.9	83	3.3	1143.1	84	3.8	7445.0	DB
7353409	2M1915+4256	11	3.4	196.3	11	3.5	884.0	11	3.8	5523.3	sdO
7755741	2M1931+4324	8	3.1	176.5	6	4.0	1126.3	7	3.8	5387.3	sdO
8619526	J19195+4445	22	3.3	328.0	22	3.8	1708.1	22	3.8	5812.1	PNN
8682822	J19173+4452	23	3.7	344.0	22	3.6	1346.4	22	3.6	6031.4	DA
9139775	J18577+4532	147	2.9	186.2	143	3.5	724.0	144	3.7	3490.4	DA
9408967	J19352+4555	High 1/*f* noise			65	3.5	1202.3	66	3.5	4954.2	He-sdOB
9583158	NSV 11917	86	3.5	498.8	81	3.5	1303.3	81	3.9	6672.5	PNN
9822180	J19100+4640	12	3.3	282.8	11	3.6	659.0	11	4.7	7444.2	sdO+F/G
9957741	J19380+4649	29	3.2	435.5	29	4.0	1162.9	28	3.6	4847.2	He-sdOB
10420021	J19492+4734	25	4.5	196.4	25	3.4	902.6	25	3.9	3748.9	DA
10482860	J19458+4739	146	3.0	123.5	145	3.7	686.1	145	3.7	5231.3	DO
11357853	J19415+4907	75	3.4	222.9	75	3.4	1116.7	76	4.1	7009.0	sdOB (Hot)
11514682	J19412+4925	25	3.4	213.3	25	3.5	942.2	25	3.5	2822.0	DAB
11822535	WD 1942+499	15	3.0	208.4	15	3.4	884.7	15	3.5	4991.4	DA

Downloaded from https://academic.oup.com/mnras/article-abstract/409/4/1470/984924 by guest on 29 April 2020

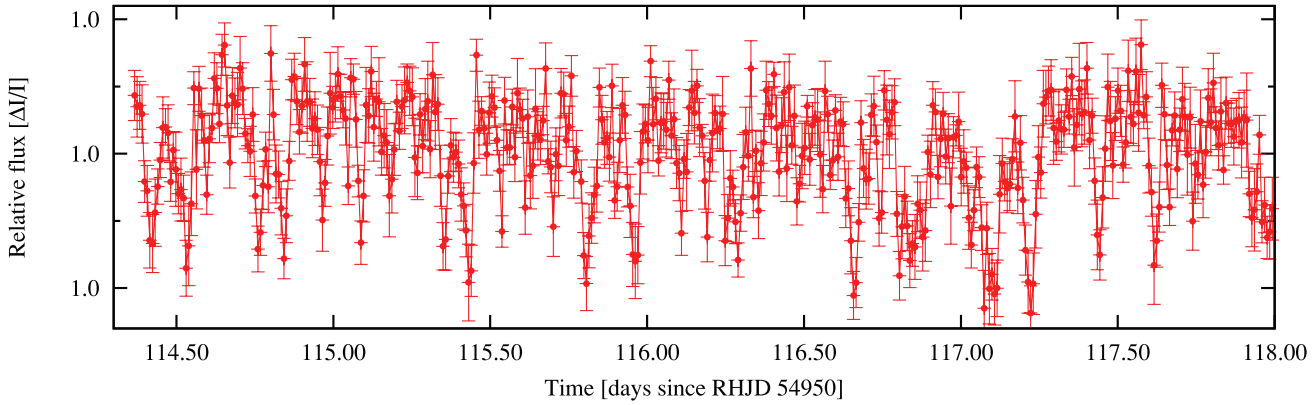

Figure 4. The light-curve of the He-sdOB J19352+4555 shows unusual dips which appears as $1/f$ noise in the FT, i.e. there is no regular recurrence. Here, only the first 3.7 d of the 1-month data set is shown. Since there is no short-term variability, the data have been binned with each point representing the average of 12 short-cadence exposures, and their rms variation.

$\sim$100 ppm for $Kp = 17.5$. Note that there are some discrepancies due to the varying contamination, which is not reflected in the *Kepler* magnitudes. The highest peak found in the FT for the targets in Table 3 lies on average around 3.7 times this level, but there are quite a few stars that show peaks between 4.0 and 4.1 times the mean. This is not unexpected considering the fact that the light curves contain around 40 000 independent measurements, and it is hard to claim that such low-amplitude pulsations are significant. However, it is worth noting that there seem to be more cases of such 4.0 times mean peaks in the sdB stars (Table 3) than in the non-sdBs (Table 5). Since the sdBs are known to show pulsations more frequently than the other classes, this may not be a coincidence, and rather an indication of low-amplitude or transient pulsation modes.

For two stars we were unable to derive useful limits in the low-frequency range. The sdB+F composite J19162+4749 shows a light curve that is not consistent with orbital motion (Fig. 8). The main variation is found at 1.9 d, far too long for a compact pulsator. We will discuss this object further in Section 4.6.

The second object with substantial power in the FT at low frequencies is the He-sdOB star J19352+4555. The light curve appears to have rapid drops in the photometry with no apparent regularity (Fig. 4), and is unlike anything we have seen in any other *Kepler* light curves. It is listed with a contamination of 80 per cent, so the variation may not be from the subdwarf, but we have no explanation for the cause.

For KBS 13 and the other low-amplitude reflection binaries we were able to subtract the orbital effect with a simple two-component sine function, to produce the limits given in Table 3. For KPD 1496+4340 we subtracted the optimal model from Bloemen et al. (2010) to produce the tabulated limits, and note that the 4.1σ peak at 5018.2 μHz is just above our significance limit.

4.4 Pulsation properties

One pulsator, KIC10139564 (J19249+4707), stands out as the only unambiguous V361 Hya pulsator in the sample, and is the subject of a dedicated paper, Paper II. While having a pulsation spectrum with substantial power in the high-frequency region, a single peak with a frequency of 315.96 μHz also appears in the FT. This is surprising, as KIC10139564 is significantly hotter than the boundary region where the DW Lyn stars are found, and much hotter than the theoretical blue edge of the g-mode instability region.

The eclipsing binary 2M1938+4603 (KIC9472174) is an especially interesting and unusual case. The pulsation spectrum is the richest of all the sdBVs and spans the whole range from 50 to 4500 μHz, something never seen before. The only other eclipsing sdB+dM system with a pulsating primary is NY Vir, so it is really an exceptional stroke of luck that the brightest EHB star among all the compact pulsator candidates is such an exceptional object. A first look at the pulsation spectrum and a detailed analysis of the binary properties is given by Østensen et al. (2010b).

The remaining seven are all multiperiodic pulsators of the V1093 Her class, and a detailed frequency analysis will be provided in two separate papers. Five objects, KIC2697388, KIC3527751, KIC7664467, KIC10670103 and KPD 1943+4058, are analysed in detail in Paper III. Interestingly, three of these show significant peaks in the short-period pulsation region, making them likely hybrid p-and-g-mode pulsators as well. For KIC3527751 and KIC5807616 this is not so much surprising, as they are close to the hot end of the g-mode region, but for KIC2697388 the presence of a short-period pulsation is unexpected, as this is the second coolest sdB star in the sample. The first asteroseismic result based on one of the stars in Paper III is presented in Paper IV, and also represents the first successful modelling of a V1093 Her star, leading through g-mode seismology to the determination of the structural and core parameters of KPD 1943+4058.

The two V1093 Her stars, KIC2991403 and KIC11179657, which clearly show a binary period in addition to their V1093 Her-type pulsation spectra are the subject of Paper V.

In Table 4 we list some general details from the frequency analysis of these pulsators, together with the physical parameters derived from our spectroscopy. In addition to the number of significant pulsation modes, the minimum and maximum pulsation frequency and the orbital period, we also provide the power-weighted mean frequency, $f_{\rm med}$. The frequency range and $f_{\rm med}$ are plotted as a function of effective temperature and gravity in Fig. 5. Roughly linear, decreasing trends are evident in pulsation period as a function of both $T_{\rm eff}$ and $\log g$, but note that $T_{\rm eff}$ and $\log g$ are highly correlated along the EHB (see Fig. 3). These eight stars all show pulsations down to the significance limit in their FTs, which means that more frequencies are likely to be discovered in longer time series. All are scheduled for three consecutive months of short-cadence observations in Q5, and will be followed closely over the full length of the *Kepler Mission*. We defer the readers to the particular studies on these objects for further details of their asteroseismic properties.

Downloaded from https://academic.oup.com/mnras/article-abstract/409/4/1470/984924 by guest on 29 April 2020

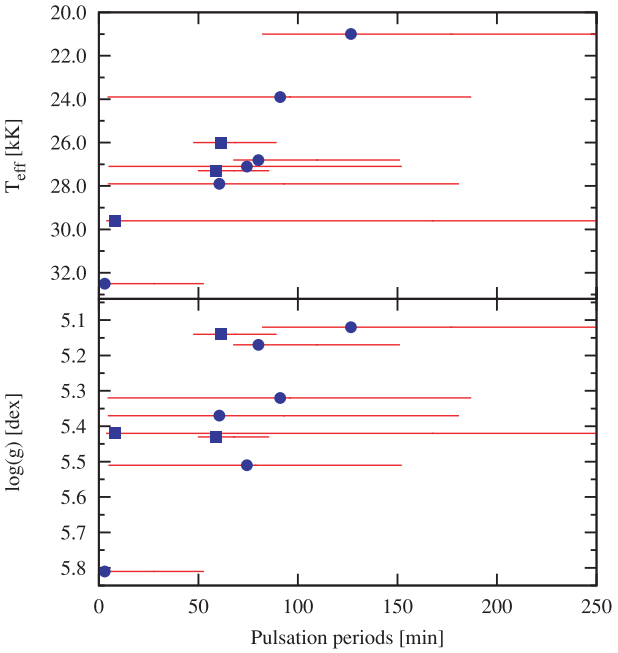

Figure 5. Pulsation periods as a function of $T_{\rm eff}$ and $\log g$ for the sdB pulsators from Table 4. The red bars indicate the range of pulsations, and the blue symbols mark the power-weighted mean frequency, $f_{\rm med}$. The three short-period binaries are marked with boxes, the rest with bullets.

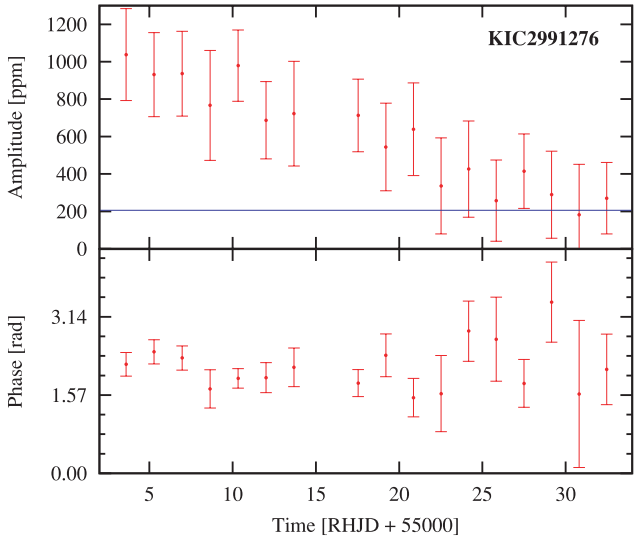

Figure 6. The transient pulsation seen in KIC 2991276. The amplitude (upper panel) and phase (lower panel) are shown for 17 roughly 1.7-d chunks of data. The line in the upper panel indicates the average of the FT noise levels in the chunks.

4.5 Transient pulsations

The FT of KIC2991276 shows a peak at 8201.1 μHz with an amplitude of 0.06 per cent, which is more than 10σ. At first we did not recognize this as a clear pulsator, as all other peaks with similarly low amplitudes in the FT are associated with known artefacts. However, no other stars show artefacts at this frequency, and since KIC2991276 was observed during the Q2.1 run, all artefacts including the one of unknown origin at 7865 μHz are double-peaked (see Section 4.2), and the 8201.1-μHz peak is not.

We examined the variability of the amplitude and phase of this signal by dividing the 1-month light curve into 17 chunks and fitting the amplitude and phase of the frequency determined from the complete data set. As Fig. 6 shows, the amplitude of the signal decreased monotonically over the time-span of the observations, whereas the phase remained constant within the errors. This argues against a beating phenomenon as the phase would be expected to vary when the amplitude approached zero.

At $P = 122$ s the true amplitude is substantially smeared during the 58.8-s integration cycle. The smearing factor is given by $\sin(x)/x$, where $x = \pi\Delta t_{\rm exp}/P$ (Kawaler et al. 1994). In our case the FT recovers ∼66 per cent of the true amplitude. But the contamination of this $Kp = 17.4$ mag star from two stars located 8 arcsec to the north ($Kp = 13.8$ and 14.2) is substantial. In the KIC $F_{\rm cont}$ is given as 0.971, but as discussed above this is most likely overestimated, since the KIC does not have the right flux distribution for UV-excess stars. Nevertheless, when the contamination and smearing are accounted for, the pulsation amplitude in the beginning of the run must be several per cent.

KIC2991276 is a normal He-poor sdB star with a temperature around 33 900 K and $\log g = 5.8$, which places it right in the middle of the instability region. Stars in this region of the instability strip often show variable amplitudes and on rare occasions transient pulsation peaks (Kilkenny 2010). A high-amplitude mode at 122 s is not unheard of, and quite comparable to the main mode in QQ Vir (Silvotti et al. 2002). Single-mode pulsators are also not unheard of in this temperature region. LS Dra was observed to have a single pulsation mode with a period of 139 s by Østensen et al. (2001a), and confirmed to be monoperiodic by Reed et al. (2006), but with a highly variable amplitude changing from a maximum of 0.526 per cent to a minimum of 0.087 per cent over their campaign spanning 47 d. Whether such an amplitude variability is due to the beating of extremely closely spaced modes, or due to true intrinsic amplitude variability requires sustained observations over a much longer period. The *Kepler Mission* is the ideal tool for accomplishing this.

4.6 Binaries and long-period variables

Five stars in our sample show clear long-period variability that we have identified as binary in origin. In addition to the three sdBs noted as pulsators in the previous section, two non-pulsators are clearly identified. Five further sdBs show variability that is unlikely to be intrinsic pulsations in the hot subdwarf, and the sdO+F/G binary shows very low-level variations at both short and long periods. We have also noted four variable systems with white dwarf primaries (see Table 6). Note that the amplitude levels are only given as an indication of the significance of the variability. They represent the peak Fourier amplitude of the raw light curves, and are affected by contamination from nearby stars, which may also be the source of the variability in some cases.

The most spectacular binary star in the sample is clearly KPD 1946+4340. This star was known to be an sdB+WD binary system from the RV study of Morales-Rueda et al. (2003), with a period of 0.4037 d and an RV amplitude of 167 km s^{-1}. The *Kepler* light curve folded on the orbital period (see top panel of Fig. 7) reveals that the object is clearly eclipsing, and shows a substantial ellipsoidal deformation superimposed on a relativistic beaming effect. A detailed study of this system is given by Bloemen et al. (2010), which presents for the first time a comparison between a radial velocity amplitude as determined from spectroscopy with one determined from photometric relativistic effects.

Downloaded from https://academic.oup.com/mnras/article-abstract/409/4/1470/984924 by guest on 29 April 2020

Table 6. Binaries and other long-period variables.

Name	Period (d)	Amp. (per cent)	Class	Main variability
KPD 1946+4340	0.404	0.5	sdB+WD	Eclipses
KBS 13	0.29	2.5	sdB+dM	Reflection effect
J19135+4302	4.24	0.3	sdB+?	Unknown
J18427+4404	1.12	1.5	sdB+?	Unknown
J19405+4827	∼1	0.1	sdB+F	Unknown
BD +42°3250	1.09	0.03	sdB?	Unknown
J19162+4749	1.9	0.9	sdB+F	Companion
J19000+4640	∼2	0.1	sdO+F/G	Companion
J18561+4537	0.17	20	DA+dM	CV
J19241+4459	0.12	20	DA+dM	CV
J19193+5044	3.67	40	DA+dMe	Flares
J19195+4445	1.12	0.05	PNN	Unknown

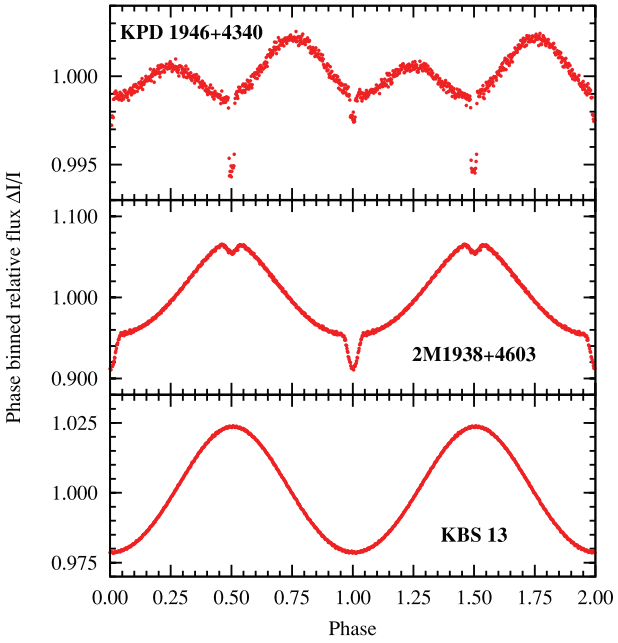

Figure 7. Three binary sdB stars. The light curves have been folded on the orbital period (P = 0.404, 0.126 and 0.29 d, respectively, top to bottom), and averaged into 500 bins. Two cycles of the orbital variation are shown.

The system 2M1938+4603 shows a light curve similar to the HW Vir systems, except that the eclipses are much more shallow, indicating that they are only grazing (Fig. 7, middle panel). This system was identified in 2008 during follow-up studies of hot subdwarfs from the 2MASS catalogue, and a first analysis of the *Kepler* data together with extensive ground-based photometry and spectroscopy is provided in Østensen et al. (2010b). The reflection binary KBS 13 (bottom panel in Fig. 7) has also been known for some time already, and details on the system were published by For et al. (2008). With an RV amplitude of only 22.8 km s^{-1}, the inclination angle must be quite small unless the secondary is substellar.

The light curve of J19162+4749 (Fig. 8) reveals substantial long-period variability, but the amplitude of the ∼1.9-d period is clearly not constant. The spectrum is composite with roughly half the optical contribution coming from an F-star companion. The target has a visible companion 5 arcsec to the east, but this star does not contribute more than ∼10 per cent of the light, and cannot be the cause of the strong contamination seen in the spectrum, so the system is

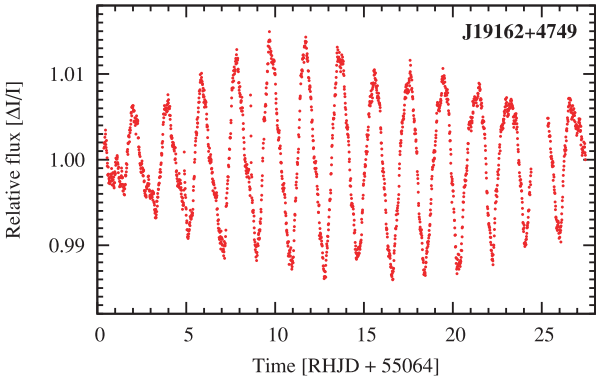

Figure 8. The light curve of J19162+4749, a strong sdB+F composite. Each point represents an average of 20 *Kepler* short-cadence observations to reduce the noise. The variability most likely comes from the F star.

most likely an unresolved binary with an early F companion. The pulsations could be from the F star, in which case it would be of the γ Doradus class, but they are sufficiently low-level that they could also be intrinsic to the contaminating star. If they were from the F star, this would be the first sdB star found to have a pulsating close companion. After concluding that there is no short-period variability in this system, we have submitted the object for further long-cadence *Kepler* photometry. If γ Doradus pulsations are confirmed in the F companion of the sdB star, asteroseismology based on 5 yr of long-cadence *Kepler* observations might shed light on the mass transfer phase where the main-sequence star most likely received most of the envelope from the sdB progenitor as it ascended the RGB.

Two more sdBs show slow amplitude modulation that might indicate a binary nature, as listed in Table 6. The clearest of these is J18427+4404 with an amplitude of ∼1.5 per cent (middle panel of Fig. 9). This star is not located in a very crowded field, but contamination cannot be completely ruled out, so a spectroscopic series to determine its radial velocity variation is required to firmly establish its binary nature. There are weak lines in the spectrum of this star that may be an indication of an F/G/K main-sequence companion, but this would be unusual as such binaries have never been seen to have short orbits. The 1.12-d period has a constant amplitude throughout the *Kepler* run, and folding the light curve on this period reveals that the light curve is not entirely symmetric, which indicates either a slightly elliptic orbit, or some kind of low-level pulsation from a main-sequence contaminating star. The same is the case for J19135+4302 (upper panel of Fig. 9) which shows an even more asymmetric cyclic variation, with a period of 4.24 d.

The sdB star J19405+4827 shows irregular variations with many different periods longer than half a day. This star is also a strong composite, so the variability could come from the companion star, possibly from starspots. Long-cadence data will be suitable to study the nature of these variations.

The same concerns about contamination apply to an even higher degree for the lower-amplitude systems with possible binary periods around 1 d. The most unlikely to suffer contamination would be the bright subdwarf BD +42°3250 (Fig. 10), as its contamination factor is only 0.003. However, the amplitude of 300 ppm is so low that a very substantial pulsation amplitude in one of the faint neighbours can be invoked to explain the observed modulation. However, BD +42°3250 is not a regular EHB star as evidenced by its low surface gravity ($\log g = 5.1$). This places it in a sparsely populated location in the $T_{\rm eff}$, $\log g$ plane, well above the canonical EHB.

Downloaded from https://academic.oup.com/mnras/article-abstract/409/4/1470/984924 by guest on 29 April 2020

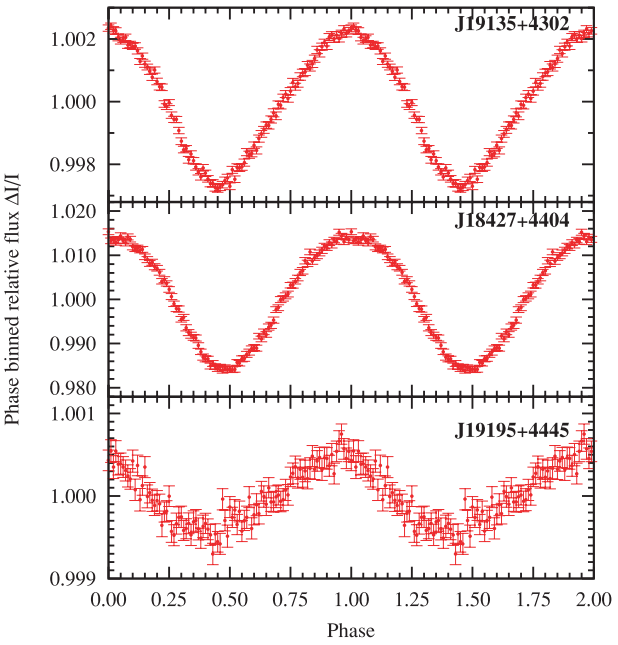

Figure 9. Three objects showing low-level variability with regular amplitude throughout the *Kepler* run. The light curves were folded on the main period ($P = 4.24$, 1.116 and 1.119 d, respectively) and binned into 100 bins to reduce the noise. The variation is either intrinsic to a companion or a contaminating field star, or an orbital variation.

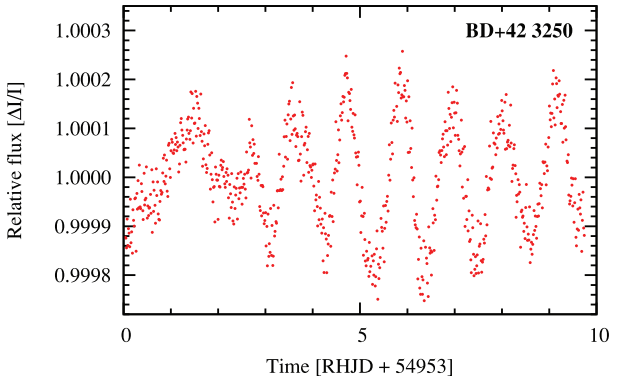

Figure 10. The light curve of BD +42°3250 shows extremely low amplitude variability with periods of around 1 d. 20 *Kepler* short-cadence observations were averaged for each point in the figure.

Post-EHB tracks for shell-burning stars only reach such low gravities when the temperature exceeds 32 000 K and post-RGB tracks require a companion in order to bypass the horizontal branch stage. Models of helium-core white dwarf mergers also pass through the hotter parts of the $T_{\rm eff}$/log g plane before reaching the EHB, but unlike BD +42°3250, these merger products are expected to display enhanced atmospheric helium at least until they settle on the EHB. Since BD +42°3250 is such an enigmatic object, the low-level variability seen in the *Kepler* photometry is worth further study.

The sdO+F/G binary J19100+4640 (KIC9822180) is a peculiar case, with significant variations on long time-scales, and a single peak at 7444.2 μHz. The long-period variations are quite irregular, more like rapidly changing starspots than harmonic pulsations, and are likely to originate from the companion or a contaminating star. The 7444.2-μHz peak is only at 4.7σ, but appears to be significant. We first suspected that it might be an hitherto undescribed instrumental artefact since one other star in Table 5 also shows its strongest high-frequency peak at 7445 μHz (but below 4σ), and the DA+dMe star (Section 4.8, below) shows it at 5.8σ. However, unlike those two WDs KIC9822180 was observed during Q2.1, and all the artefacts associated with the readout cycles are double peaked, as discussed in Section 4.2. The 7444.2-μHz peak is single-peaked and is therefore very likely to originate from the target.

4.7 Cataclysmic variables

The light curves of the two objects identified as CVs from the spectroscopy (Fig. 2) both show substantial levels of activity (top two panels of Fig. 11). J18561+4537 shows a light curve dominated by long-term variations. Superimposed on these trends is a regular oscillation with a period of 0.166 d with a peculiar sawtooth shape. We interpret this as the orbital period since it is typical of nova-like variables, whereas half of that period would be exceptionally short. In fact, J18561+4537 is remarkably similar in terms of its spectrum, orbital period and low-amplitude orbital modulation to a number of known nova-like variables (Aungwerojwit et al. 2005). As the spectrum is disc-dominated, the large variability seen in the light curve both on short and long time-scales must originate from the disc or the bright-spot where the gas stream hits the disc. The long period could be ascribed to the precessional behaviour of the outer disc, but could also be due to variations in the mass-transfer rate. However, due to the strong similarity between cycles, the latter is less likely. One can also clearly distinguish a modulation of the orbital signal with the long-period variation, which is consistent with precessional behaviour changing the viewing angle and therefore the projected brightness of the hotspot. Time-resolved spectroscopy and Doppler tomography have the potential to map the structure of the disc, and the precessional cycle will permit several viewing angles of the system that could reveal interesting details on accretion disc physics.

The second object, J19241+4459, is a nova-like CV of the UX UMa class in or near the period gap, and it may be a new member of the rapidly growing subclass of SW Sex systems (Williams et al. 2010). The FT is dominated by the period at 0.122 d, interpreted as the orbital period, and its harmonics.

At least 11 cataclysmic variables are known to have pulsating primaries of the ZZ Ceti type (Szkody et al. 2009). However, neither of our CVs shows any clear signs of such pulsations. But in both systems the disc is very bright, and the WD most likely contributes no more than ∼1 per cent of the flux. All the ZZ Ceti pulsators in CVs detected to date have been found in low mass transfer systems, and the WDs in nova-like variables are usually too hot for ZZ Ceti-type pulsations. However, with the unprecedented precision of sustained *Kepler* photometry, pulsations might still be detected. Note also that Szkody et al. (2010) have recently established that the instability strip for DA pulsators in CVs extends to 15 000 K, substantially hotter than for normal single ZZ Ceti stars.

4.8 A DA with a flaring companion

The light curve shown in the bottom panel of Fig. 11 is dominated by brief flares, typical of a chromospherically active M-dwarf star. While our original spectroscopic classification based on the ISIS blue arm spectrum shows the broad absorption features of a single DA white dwarf, extracting the red-arm spectrum clearly reveals the signature absorption bands of a red dwarf, and with the sharp Hα emission feature that usually indicates chromospheric activity. The sinusoidal modulation with a period of 3.655 d and an amplitude

Downloaded from https://academic.oup.com/mnras/article-abstract/409/4/1470/984924 by guest on 29 April 2020

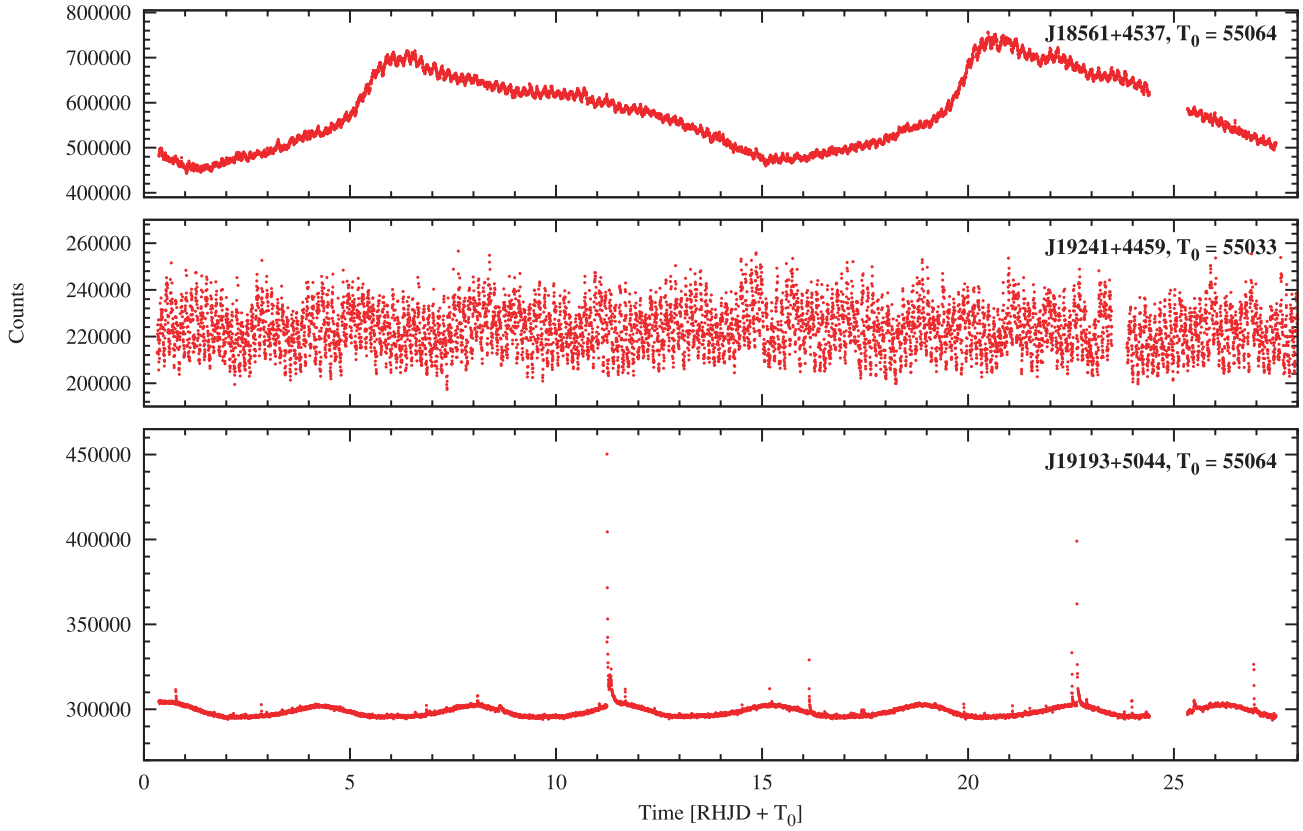

Figure 11. High amplitude variable compact objects in binary systems.

of ∼1.1 per cent could well be the orbital period, but it might also be the rotation period of the M-dwarf, as spots are expected to be associated with the flares.

Interestingly, after cleaning out the 3.655-d period and its harmonic, and sigma filtering the detrended light curve to remove most of the flares, we were able to reduce the mean noise level in the FT to 29 ppm. A peak at 5016.7 μHz is then found at 7.1 times the noise level. This peak remains significant if the data are split into two halves, and processed independently. A second peak is also found at 7444.9 μHz at 5.8 times the noise level. Thus, the WD primary in KIC12156549 might be a low-level pulsator.

A calibrated version of the WHT/ISIS blue+red-arm spectrum is shown in Fig. 12 together with the 2MASS IR magnitudes ($J = 12.950 \pm 0.026$, $H = 12.442 \pm 0.030$, $K = 12.141 \pm 0.020$), and the model spectrum of a DA white dwarf with an effective temperature of ∼20 000 K and an M3 secondary. The *JHK* colours can also be used directly to estimate the spectral type for the companion, since the WD contribution is very low in the IR. Following Hoard et al. (2007) we find that a spectral type of M4 gives the best match, but M3 would require only a reduction in $H - K$ of 0.02, which is reasonable considering the blue slope of the WD flux seen in Fig. 12, so we conclude that the companion is most likely of class mid-M3 with M3.0 to M4.0 as a plausible range. M3 would place the system at a distance of ∼140 pc, while M4 puts it at ∼100 pc. Assuming a mass of the white dwarf of 0.6 $M_\odot$, and taking the *B* magnitude to be 16.0, implies that the WD temperature must be 24 000 K for 140 pc and 18 000 K for 100 pc. 24 000 K is at the border of what is acceptable based on the width of the Balmer lines in the blue spectrum, so we adopt this range as our current best estimate for the WD temperature, $T_{\rm eff} = 21\,000 \pm 3\,000$ K. Given the relatively low temperature of the WD, the observed 3.65-d modulation is unlikely to be caused by irradiation effects. A more likely hypothesis is that it is caused by spots on the surface of the M-dwarf, and that the 3.65-d period represents its rotation rather than the orbital period.

Our temperature range for the WD primary shows that it is too hot to be a regular ZZ Ceti pulsator, since that type of instability only occurs inside an exclusive strip between 11 000 and 12 500 K. Kurtz et al. (2008) discuss candidate DA pulsators residing in the DB gap between 30 000 and 45 000 K, but excited by the same mechanism that drives pulsations in the V777 Her stars (or DBVs). These stars would be structurally similar to the DB stars, but with a thin hydrogen envelope making them appear spectroscopically as DA white dwarfs. The temperatures of the known V777 Her stars span the range between 21 800 and 27 800 K. It is an intriguing possibility that the DA primary in J19193+5044 could be a WD that normally would appear as a DB star if not for a thin hydrogen shell. An envelope mass of between 10^{-15}–10^{-16} $M_\odot$ is all that is required to make a helium-atmosphere white dwarf appear as a DA (Koester & Chanmugam 1990), and the WD in J19193+5044 could accrete such an amount of hydrogen from the circumbinary envelope produced by the flaring M-dwarf.

Since the amplitudes of the pulsation peaks found in the *Kepler* photometry of KIC12156549 are at the 200 ppm level, a region never before explored for white dwarfs, it may not really make sense to confine ourselves to the regular instability strips for known classes of white dwarf pulsators. At these low amplitudes we may be seeing the signature of excited pulsation modes of $\ell > 2$, that are subject to substantial geometric cancellations. Such stars may be inhabiting temperature regions where pulsations in the readily observable $\ell = 1,2$ modes are damped, and therefore outside the

Downloaded from https://academic.oup.com/mnras/article-abstract/409/4/1470/984924 by guest on 29 April 2020

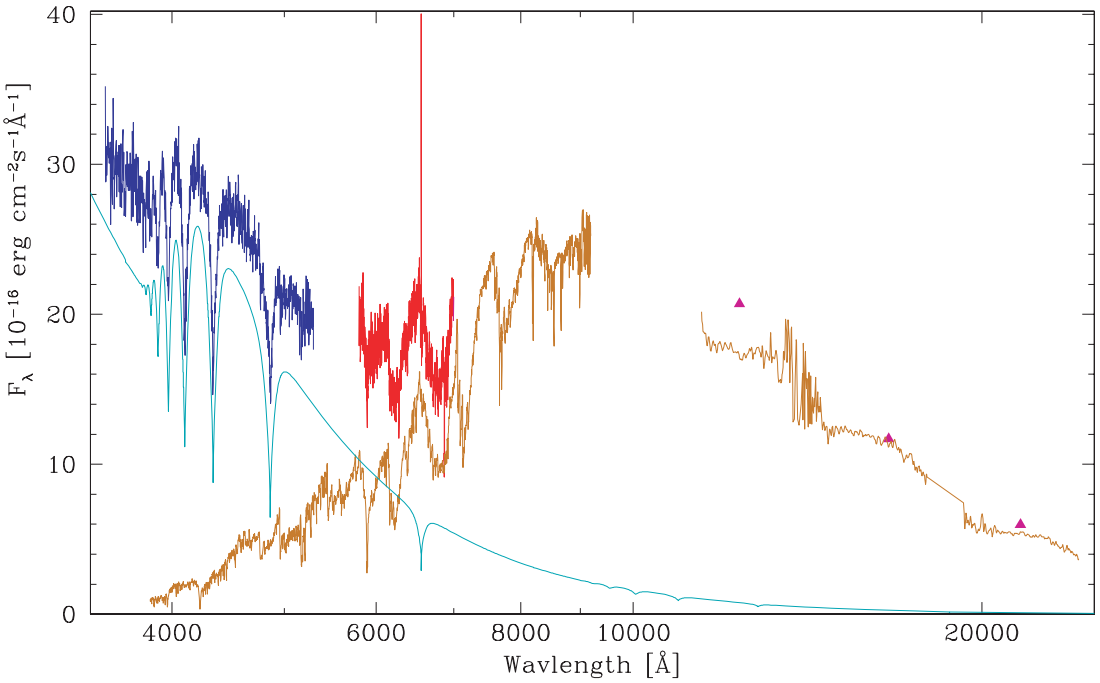

Figure 12. Spectral energy distribution for J19193+5044. The WHT/ISIS spectra from the blue and red arm are shown as blue and red curves, and the 2MASS *JHK* fluxes are indicated by triangles. The lower curves show model spectra for a 20 000 K DA white dwarf (light blue), and an M3 red dwarf (brown).

regular instability strips. Since we are exploring uncharted territory we will refrain from further speculation until the next cycle of *Kepler* photometry can confirm the pulsations, and our ongoing spectroscopy has established the orbit and placed useful limits on the masses of the binary components of the system.

5 CONCLUSIONS

In the first four months of the survey phase (plus 10 d of commissioning), *Kepler* has observed 63 compact pulsators candidates and found nine unambiguous subdwarf B pulsators: seven belonging to the V1093 Her class (long periods), including several with hybrid behaviour, one rapid pulsator of the V361 Hya type also showing a single long-period mode, indicating low-level hybrid behaviour, and one unusual hybrid pulsator in an eclipsing sdB+dM binary. Including the transient pulsator with a single vanishing pulsation mode means that we have discovered 10 new sdBV stars in the first half of the *Kepler* survey phase.

No clearly pulsating white dwarfs were detected in this part of the survey, but two candidate WD pulsators with extremely low amplitudes have been submitted for further *Kepler* observations. More intriguing is the likely detection of low-amplitude pulsations that could originate from the white dwarf component of the DA+dMe binary J19193+5044. Being substantially hotter than the classic ZZ Ceti instability strip, this object certainly merits further investigations. The DAV candidate KIC10420021 and the sdOV candidate KIC9822180 are both very marginal detections, at $\sim 4.5\sigma$, and both require further observations before firm conclusions can be made.

If the statistics on the sdB pulsators hold up, the total number of pulsators at the completion of the survey phase could be 18. This number is not far from what was expected (Silvotti 2004); a number of about 10 and 2–3 was expected for the sdBV and DAV pulsators, respectively, when considering a *Kepler* magnitude limit of 17.5. However, there are at least two differences. The first being that the number of long-period sdB pulsators is higher than expected. As pointed out in Section 3.2, this is due to the fact that the fraction of pulsating sdBs in the long-period instability strip is formally 100 and not 50 per cent, as in our original conservative estimate. The second difference is that, contrary to the expectations, no true DAVs have been detected in this half of the sample. Due to their intrinsic faintness, all the DA white dwarfs observable with *Kepler* belong to the Galactic disc, implying that the number of DAVs inside the *Kepler* FoV is highly dependent on the magnitude limit (while this is only marginally true for sdBs that are mostly outside the disc at the faint end of our sample). The number of DAVs potentially observable with *Kepler* increases by a factor 4 when increasing the limiting magnitude by 1. Pushing the magnitude limit to 19.5 (which would still be acceptable with respect to the photometric accuracy), we could expect about 40 DAVs in the *Kepler* FoV. In the first 4 months, only seven spectroscopically confirmed DAs were observed, and in the months that remain our survey shows only six more DAs and one single DB, leaving us cautiously optimistic that at least one WD pulsator will be found in the final months of the survey phase.

An unexpected result is the observation that of the 12 stars in Fig. 3 that lie in the EHB at temperatures above 28 000 K, only two are clearly pulsating, and only one of the remainder shows any trace of variability. We had expected that the ∼10 per cent pulsator fraction found in ground-based surveys would increase substantially with the much extended time-base and reduced noise level of *Kepler* observations, but 25 per cent goes some of the way. That nine out of 12 sdB stars in the V361 Hya instability region do not show any trace of pulsational instability is therefore an enduring enigma.

The detection of at least one clearly transient pulsator is a welcome discovery, corroborating for the first time the pulsation episode discussed by Piccioni et al. (2000) in HK Cnc (PG 0856+121). Jeffery & Saio (2007) speculated that the iron-group element enhancements, which build up due to a diffusion process over rather long time-scales, may be disrupted by the atmospheric motions when pulsations reach sufficient levels. They note

Downloaded from https://academic.oup.com/mnras/article-abstract/409/4/1470/984924 by guest on 29 April 2020

that since *p*-modes mostly involve vertical motion, while *g*-modes are dominated by horizontal motion, it is possible that *p*-modes are more effective at redistributing the iron-group elements out of the driving zone. In this way, it may be the pulsations themselves that conspire to suppress the driving mechanism. However, it is hard to understand how this process can act so rapidly as we observe here, when the typical diffusion time-scales are 10^5–10^6 yr. Another possible explanation was recently suggested by Théado et al. (2009), in which iron-group enhanced layers lying on the top of light elements will lead to 'iron fingers', which are similar to the so-called 'salt fingers' that are linked to the thermohaline convection in the oceans. Such convection can occur on time-scales of a few thousand years, much shorter than classical diffusion. More work is definitely warranted both on the theoretical and on the observational side in order to better understand the incidence and diversity in pulsation power found in the subdwarf B pulsators. It would be worthwhile to revisit the sdB stars in Table 3 later in the mission in order to search for further transient pulsation events, and to determine how common they are.

In this paper we have focused mostly on the many interesting sdB stars in the compact pulsator sample. While there have been some intriguing low-level photometric amplitudes detected in a few of the white dwarf stars in the sample, we have not given these stars the detailed treatment they deserve. After the final survey data have been released and processed, we will subject the complete set of white dwarf spectra to atmospheric analysis and discuss them together with the photometric analysis of the second half of the compact star sample.

Whereas the *Kepler Mission* has just begun, it has already lived up to its expectations both in providing photometric data of unprecedented quality and duration on known types of compact pulsators, as well as revealing new and unexpected short-period phenomena. We eagerly await the forthcoming release of the remaining half of the survey phase, as well as the results that will come with another order-of-magnitude increase in photometric precision that can be reached on targets selected for study throughout the remainder of the mission.

ACKNOWLEDGMENTS

The authors gratefully acknowledge the *Kepler* team and everybody who has contributed to making this mission possible. Funding for the *Kepler Mission* is provided by NASA's Science Mission Directorate.

The research leading to these results has received funding from the European Research Council under the European Community's Seventh Framework Programme (FP7/2007–2013)/ERC grant agreement Nº 227224 (PROSPERITY), as well as from the Research Council of K.U.Leuven grant agreement GOA/2008/04. ACQ is supported by the Missouri Space Grant Consortium, funded by NASA.

We thank Alexander Brown (University of Colorado) for giving us early access to the *Galex* GO observations of the *Kepler* field.

For the spectroscopic observations presented here we acknowledge the Bok Telescope on Kitt Peak, operated by Steward Observatory, the Nordic Optical Telescope at the Observatorio del Roque de los Muchachos (ORM) on La Palma, operated jointly by Denmark, Finland, Iceland, Norway, and Sweden, and the William Herschel and Isaac Newton telescopes also at ORM, operated by the Isaac Newton Group.

Facilities: *Kepler*.

REFERENCES

Abell G. O., 1966, ApJ, 144, 259
Abrahamian H. V., Lipovetski V. A., Mickaelian A. M., Stepanian J. A., 1990, Afz, 33, 213
Aerts C., Christensen-Dalsgaard J., Kurtz D. W., 2010, Asteroseismology. Springer, Berlin
Aungwerojwit A. et al., 2005, A&A, 443, 995
Baran A., Fox Machado L., 2010, Ap&SS, in press
Blanchette J., Chayer P., Wesemael F., Fontaine G., Fontaine M., Dupuis J., Kruk J. W., Green E. M., 2008, ApJ, 678, 1329
Bloemen S. et al., 2010, MNRAS, in press (doi:10.1111/j.1365-2966.2010.17559.x)
Borucki W. J. et al., 2010, Sci, 327, 977
Bryson S. T. et al., 2010, ApJ, 713, L97
Charpinet S., Fontaine G., Brassard P., Chayer P., Rogers F. J., Iglesias C. A., Dorman B., 1997, ApJ, 483, L123
Charpinet S., Brassard P., Fontaine G., Green E. M., van Grootel V., Randall S. K., Chayer P., 2009, in Guzik J. A., Bradley P. A., eds, AIP Conf. Ser. Vol. 1170, Progress in Sounding the Interior of Pulsating Hot Subdwarf Stars. Am. Inst. Phys., New York, p. 585
Downes R. A., 1986, ApJS, 61, 569
Edelmann H., Heber U., Hagen H.-J., Lemke M., Dreizler S., Napiwotzki R., Engels D., 2003, A&A, 400, 939
Edelmann H., Heber U., Napiwotzki R., 2006, Baltic Astron., 15, 103
Fontaine G., Brassard P., Charpinet S., Green E. M., Chayer P., Billères M., Randall S. K., 2003, ApJ, 597, 518
Fontaine G., Brassard P., Charpinet S., Chayer P., 2006, Mem. Soc. Astron. Italiana, 77, 49
For B., Edelmann H., Green E. M., Drechsel H., Nesslinger S., Fontaine G., 2008, in Heber U., Jeffery C. S., Napiwotzki R., eds, ASP Conf. Ser. Vol. 392, Hot Subdwarf Stars and Related Objects. Astron. Soc. Pac., San Francisco, p. 203
Geier S., Heber U., Edelmann H., Morales-Rueda L., Napiwotzki R., 2010, Ap&SS, in press
Gilliland R. L. et al., 2010a, PASP, 122, 131
Gilliland R. L. et al., 2010b, ApJ, 713, L160
Green E. M. et al., 2003, ApJ, 583, L31
Heber U., 2009, ARA&A, 47, 211
Heber U., Reid I. N., Werner K., 2000, A&A, 363, 198
Hoard D. W., Wachter S., Sturch L. K., Widhalm A. M., Weiler K. P., Pretorius M. L., Wellhouse J. W., Gibiansky M., 2007, AJ, 134, 26
Jeffery C. S., Saio H., 2007, MNRAS, 378, 379
Kawaler S. D., Bond H. E., Sherbert L. E., Watson T. K., 1994, AJ, 107, 298
Kawaler S. D. et al., 2010a, MNRAS, in press (doi:10.1111/j.1365-2966.2010.17528.x) (Paper II, this issue)
Kawaler S. D. et al., 2010b, MNRAS, in press (doi:10.1111/j.1365-2966.2010.17475.x) (Paper V, this issue)
Kilkenny D., 2010, Ap&SS, in press
Kilkenny D., Koen C., O'Donoghue D., Stobie R. S., 1997, MNRAS, 285, 640
Kilkenny D., Fontaine G., Green E. M., Schuh S., 2010, Inf. Bull. Var. Stars, 5927, 1
Koester D., Chanmugam G., 1990, Rep. Progress Phys., 53, 837
Kronberger M. et al., 2006, A&A, 447, 921
Kurtz D. W., Shibahashi H., Dhillon V. S., Marsh T. R., Littlefair S. P., 2008, MNRAS, 389, 1771
Lutz R., Schuh S., Silvotti R., Bernabei S., Dreizler S., Stahn T., Hügelmeyer S. D., 2009, A&A, 496, 469
Marsh M. C. et al., 1997, MNRAS, 286, 369
Martin D. C. et al., 2005, ApJ, 619, L1
Montgomery M. H., Williams K. A., Winget D. E., Dufour P., De Gennaro S., Liebert J., 2008, ApJ, 678, L51
Morales-Rueda L., Maxted P. F. L., Marsh T. R., North R. C., Heber U., 2003, MNRAS, 338, 752
Napiwotzki R., 1997, A&A, 322, 256
Napiwotzki R., 1999, A&A, 350, 101

Downloaded from https://academic.oup.com/mnras/article-abstract/409/4/1470/984924 by guest on 29 April 2020

O'Toole S. J., Heber U., 2006, A&A, 452, 579
Oreiro R., Ulla A., Pérez Hernández F., Østensen R., Rodríguez López C., MacDonald J., 2004, A&A, 418, 243
Oreiro R., Pérez Hernández F., Ulla A., Garrido R., Østensen R., MacDonald J., 2005, A&A, 438, 257
Østensen R., 2009, Comm. Asteroseismol., 159, 75
Østensen R., Heber U., Silvotti R., Solheim J.-E., Dreizler S., Edelmann H., 2001a, A&A, 378, 466
Østensen R., Solheim J.-E., Heber U., Silvotti R., Dreizler S., Edelmann H., 2001b, A&A, 368, 175
Østensen R. H. et al., 2010a, A&A, 513, A6
Østensen R. H. et al., 2010b, MNRAS, 408, L51
Piccioni A. et al., 2000, A&A, 354, L13
Podsiadlowski P., Han Z., Lynas-Gray A. E., Brown D., 2008, in Heber U., Jeffery C. S., Napiwotzki R., eds, ASP Conf. Ser. Vol. 392, Hot Subdwarf Stars and Related Objects. Astron. Soc. Pac., San Francisco, p. 15
Ramsay G., Napiwotzki R., Hakala P., Lehto H., 2006, MNRAS, 371, 957
Randall S. K. et al., 2006, ApJ, 645, 1464
Reed M. D., Eggen J. R., Zhou A.-Y., Terndrup D. M., Harms S. L., An D., Hashier M. A., 2006, MNRAS, 369, 1529
Reed M. et al., 2010, MNRAS, in press (doi:10.1111/j.1365-2966.17423.x) (Paper III, this issue)
Schuh S., Huber J., Dreizler S., Heber U., O'Toole S. J., Green E. M., Fontaine G., 2006, A&A, 445, L31
Silvotti R., 2004, in Favata F., Aigrain S., Wilson A., eds, ESA SP-538, Stellar Structure and Habitable Planet Finding. ESA, Paris, p. 141
Silvotti R., Østensen R., Heber U., Solheim J.-E., Dreizler S., Altmann M., 2002, A&A, 383, 239
Silvotti R. et al., 2006, A&A, 459, 557
Silvotti R. et al., 2007, Nat, 449, 189
Silvotti R., Handler G., Schuh S., Castanheira B., Kjeldsen H., 2009, Communications Asteroseismol., 159, 97
Skrutskie M. F. et al., 2006, AJ, 131, 1163
Stoughton C. et al., 2002, AJ, 123, 485
Szkody P., Mukadam A. S., Gänsicke B. T., Henden A., Nitta A., Sion E. M., Townsley D., 2009, in Murphy S. J., Bessell M. S., eds, ASP Conf. Ser. Vol. 404, The Eighth Pacific Rim Conference on Stellar Astrophysics: A Tribute to Kam Ching Leung. Astron. Soc. Pac., San Francisco, p. 229
Szkody P. et al., 2010, ApJ, 710, 64
Théado S., Vauclair S., Alecian G., Le Blanc F., 2009, ApJ, 704, 1262
Van Grootel V. et al., 2010, ApJ, 718, L97, (Paper IV)
Williams K. A. et al., 2010, AJ, 139, 2587
Woudt P. A. et al., 2006, MNRAS, 371, 1497
Yanny B. et al., 2009, AJ, 137, 4377

This paper has been typeset from a TEX/LATEX file prepared by the author.

Downloaded from https://academic.oup.com/mnras/article-abstract/409/4/1470/984924 by guest on 29 April 2020